CHALMERS

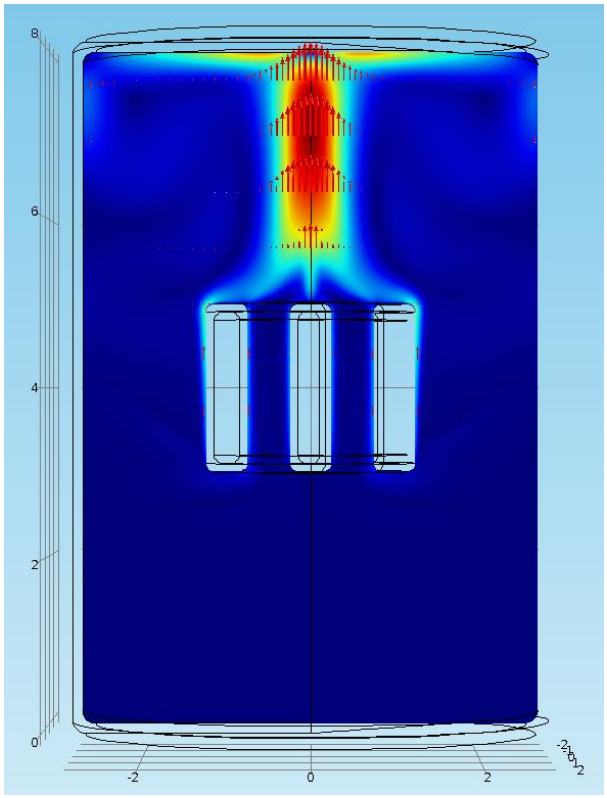

Sensible heat storage in a water tank

Influence of the heat source location and the height of the tank on the temperature distribution

Degree Project in the Engineering Programme Building and Civil Engineering

BENJAMIN BELLO
CHARLINE LEGER

Department of Civil and Environmental Engineering
Division of Building Technology
Building Physics Group
CHALMERS UNIVERSITY OF TECHNOLOGY
Göteborg 2014
Degree project 2014:15

DEGREE PROJECT 2014:15

Sensible heat storage in a water tank

Influence of the heat source location and the height of the tank on the temperature distribution

Degree project in the Engineering Programme Building and Civil Engineering

BENJAMIN BELLO

CHARLINE LEGER

Department of Civil and Environmental Engineering
Division of Building Technology

Building Physics Group
CHALMERS UNIVERSITY OF TECHNOLOGY

Göteborg, 2014

Sensible heat storage in a water tank

Influence of the heat source location and the height of the tank on the temperature distribution

Degree project in the Engineering Programme Building and Civil Engineering

BENJAMIN BELLO
CHARLINE LEGER

Examensarbete / Institutionen för bygg- och miljöteknik,
Chalmers tekniska högskola 2014:15

Department of Civil and Environmental Engineering
Division of Building Technology
Building Physics Group
Chalmers University of Technology
SE-412 96 Göteborg
Sweden
Telefon: 031-772 10 00

Cover:
Print screen of a COMSOL simulation which shows the velocity profile within a tank heated by three heating devices placed in the middle.

Department of Civil and Environmental Engineering
Göteborg 2014

Sensible heat storage in a water tank

Influence of the heat source location and the height of the tank on the temperature distribution

Degree project in the Engineering Programme Building and Civil Engineering

BENJAMIN BELLO

CHARLINE LEGER

Department of Civil and Environmental Engineering
Division of Building Technology
Building Physics Group
Chalmers University of Technology

ABSTRACT

Supermarkets need refrigerating devices to keep a cold enough ambiance inside the cabinets. A significant amount of heat is released during the condensation stage of the refrigerating process implemented. Instead of wasting this available energy, it is possible to store it at a certain temperature. The study deals with the sensible heat storage and the storing medium consists of an insulated water tank where the water is heated from 20°C towards 35°C by a heat source representing the heat pumps´ condenser.

Regarding sensible heat storage in water tanks, two parameters which can affect the vertical stratification are considered in this report. The purpose is to study how the location of the heat source and the height of the tank influence the temperature distribution.

In order to compute the process inside the tank, CFD simulations are run on COMSOL as a combined fluid dynamics and heat transfer model. The study begins with a simplified case where a Dirichlet condition is set on the edges of the tank in order to have a first overview of the phenomenon. Afterwards, more complex studies on the heat source location are carried out to investigate the effect on the temperature distribution when the heat source is immersed. The results show that setting the heating devices on the bottom fosters the temperature homogenization inside the tank and allows having a large amount of hot water available. The configuration where the heat source is on the top of the tank creates a high temperature gradient from the bottom to the top and limits the amount of hot water available. The height of the tank is the last parameter studied and it proves that among several tanks having the same volume, the higher the tank is, the more pronounced the stratification is.

Key words: Sensible heat energy storage, water tank, turbulent flow, fluid dynamics, COMSOL, temperature distribution, vertical stratification

Contents

ABSTRACT I
CONTENTS III
PREFACE VI
NOTATIONS VII

1. INTRODUCTION 1
1.1 Objective and scope 1
1.2 Method 2
1.3 Boundaries and assumptions of the study 3

2. DESCRIPTION OF THE STUDY 5
2.1 The vapor compression process 5
2.2 Model properties 5
2.2.1 Water properties 6
2.2.2 Parameters used 8
2.3 Physical model 8
2.3.1 Dimensionless numbers 8
2.3.2 Turbulent flow model 9
2.4 Model inputs 10
2.4.1 Non-slippery boundary condition 10
2.4.2 Initial values 10
2.4.3 Volume force and pressure constraint point 11
2.4.4 External boundaries 11
2.4.5 Heat transfer in solids 11
2.4.6 Heat and flow symmetry 12
2.4.7 Definition of the mesh 12
2.4.8 Physics involved 13

3. HEAT SOURCE ON THE EDGES OF THE WATER TANK 14
3.1 Position of the heat source 14
3.2 Method 15
3.3 Results 15
3.3.1 Temperature profiles 16
3.3.2 Input power 17

4. HEAT SOURCE IMMERSED INSIDE THE WATER TANK 18
4.1 Equal space interval plates model 18
4.1.1 Definition of the model 18
4.1.2 Method 19
4.1.3 Results 19
4.2 Model of remote plates 23

4.2.1 Definition of the model 23
4.2.2 Results 24

5. INFLUENCE OF THE HEIGHT OF THE TANK ON THE VERTICAL STRATIFICATION 26

5.1 2D model 26
5.1.1 Choice of the cut lines 26
5.1.2 Temperature profiles 29

5.2 2D axi-symmetrical model 30
5.2.1 Choice of the cut lines 31
5.2.2 Temperature profiles 32
5.2.3 Input power 36
5.2.4 Velocity profiles 37

CONCLUSION 41

APPENDIX A – SPECIFIC HEAT CAPACITIES FOR SEVERAL MATERIALS 42

APPENDIX B – AVAILABLE HEAT POWER AT THE CONDENSER OVER THE TIME 43

APPENDIX C – DETERMINATION OF THE OPTIMUM INSULATION LAYER 46

APPENDIX D – INFLUENCE OF THE HEAT SOURCE TEMPERATURE ON THE STRATIFICATION 48

APPENDIX E – STUDY ON THE REFRIGERATING CYCLE FOR THE SETTING OF T_{HEAT} VALUE 50

APPENDIX F – TOWARDS THE STUDY WHEN ADDING AN INLET OF HOT WATER 53

BIBLIOGRAPHY 55

REFERENCES 56

Preface

In this project, numerical models of hot water tanks have been simulated in order to study the effect of the location of the heat source and the height of the tank on the temperature distribution.

The project was initiated in Chalmers University of Technology on January 20th 2014 for a period of eleven weeks and was supervised by Tommie Månsson, PhD student at the Division of Building Technology in the Department of Civil and Environmental Engineering and York Ostermeyer, Assistant Professor at the Division of Building Technology in the Department of Civil and Environmental Engineering.

We would like to thank Tommie Månsson for his patience, the time he allowed us, his advice and his knowledge of COMSOL, which was very helpful since we encountered many simulation problems. We would also like to thank our colleagues, Carlos Mora, Staffan Sjöberg and Duncan Watt for their good mood and their support.

Göteborg, 2014

Benjamin Bello

Charline Leger

Notations

Latin uppercase letters

COP	Coefficient of performance, [-]
Gr	Grashof number, [-]
P	Pressure, [Pa]
T	Temperature, [^{o}C]

Latin lowercase letters

c_p	Specific heat capacity, [J/(kg.K)]
g	Acceleration of gravity, [m/s^2]
h	Enthalpy, [J/kg]
u	Fluid velocity, [m/s]
t	Time, [s]

Greek lowercase letters

β	Coefficient of volume thermal expansion, [K^{-1}]
λ	Thermal conductivity, [W/(m.K)]
ρ	Density, [kg/m^3]
μ	Dynamic viscosity, [kg/(m.s)]

Abbreviation

CFD	Computational Fluid Dynamics

1. Introduction

Supermarkets shelter many chilled (4°C) and cold (-18°C) cabinets to keep the food at the right and sanitary temperature conditions. To create and maintain cold inside the cabinets, refrigerating systems are running continuously. This refrigeration process represents almost 50% (Arias, 2005) of the overall electrical energy usage of supermarkets, in Sweden.

These machines consist of heat pumps which extract heat from the cold cabinets. This process releases heat at the condensers due to changing phase during the condensation from gas to liquid. Based on common models performing a COP of 3, the amount of this waste heat is significant because directly linked to the electrical consumption of the compressors. That is why it seems interesting to collect this energy instead of wasting it. The supermarket could be used as a buffer for a housing estate or a greenhouse for instance. This waste heat remains at a low temperature and can be used in a low temperature space heating system or to pre-heat hot water.

First of all and in order to deliver it afterwards, the heat has to be stored at a certain temperature. Thus, the idea of this project work is to study a way of collecting and storing this waste heat in order to have a stock available at any time.

1.1 Objective and scope

The general issue can be seen through three main steps:

- First, calculating the accurate shifting of the heat power released each day and be able to estimate the amount of heat introduced in the tank along the day. This step consists of collecting data and estimating by hand calculations.
- Then, studying the storage stage itself to study how the heat is collected and stored. On this step, it is possible to go more into details and see how the process works within the storing medium. This one can be done through dynamic simulations.
- Finally, finding a possible implementation for this heat. This work consists of developing heat distribution and means to exchange the heat from the tank towards the users.

The aim of such a project is above all using COMSOL to implement CFD calculations involving fluid mechanics and heat transfers. That is why the project is focused on the second step, more precisely on the sensible way to recover the waste heat rejected from the condensers. This process is based on the temperature change of a substance, that is to say its temperature rises when it is subject to a heat source. Regarding heat storage, the better is the specific mass heat capacity of the substance, the more heat can be stored per unit of weight.

The sensible heat energy from a material is given by:

$$\mathrm{Q_{sensible}} = \int_{T_1}^{T_2} \rho(\mathrm{T}) * \mathrm{V} * \mathrm{Cp}(\mathrm{T})\, dT \qquad (1)$$

Moreover, among many liquid substances, liquid water presents the highest heat capacity (*see Appendix A*), that is why liquid water is here used as the heat storing element and the whole system consists of an insulated water tank.

When the water is heating up, vertical water stratification occurs due to water masses with different temperatures which form layers that act as barriers to water mixing. These layers are normally arranged according to their density, with the least dense water masses sitting above the denser layers.

Finally, this project is a way to visualize through numerical simulations the basic physics phenomena involved when thinking of hot water movements and convection inside a tank. To this end, the main purpose is to analyze how the location of the heat source can influence the vertical stratification inside the water tank and how the height of the tank affects the temperature distribution.

1.2 Method

The dynamic simulations will allow visualizing the behavior of hot water and temperature distribution inside a tank in terms of velocity field evolution, temperature profiles and input power involved. It will enable to understand how these parameters are correlated to each other.

The idea is to start with simple cases where the heat source is set on the boundaries to model a source placed either on the bottom, on the top, on the side or even in the middle of the bottom part of the tank. This can be related to a hot plate heating up the water inside a boiler. This step should enable us to more understand the global process and have a first approach regarding the coil location influence.

Then, the process will lead towards a more realistic model taking into account the geometry of the coil by modeling several plates inside the tank in order to increase the exchange area. No inlet nor outlet mass flow are implemented, and the tank is considered as a closed system without any flow perturbation inside. The idea is to only study the stratification phenomenon in an ideal case.

All these simulations are done in 2D in order to visualize the velocity field and the temperature profile on a vertical plan in the middle section of the tank. For some issues regarding the tank height influence for instance, the problem is carried out on an axi-symmetrical 2D model which gives results on a 3D geometry afterwards.

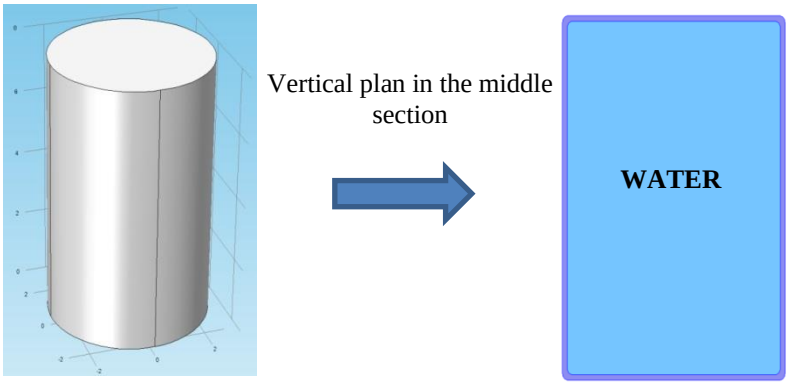

Figure 1.1: 3D model of the tank and its vertical middle section

In order to decrease the time calculations, most of the simulations are modeled with symmetry. However, it happened sometimes that building models which include symmetry led to convergence problems on COMSOL. Thus, it was necessary to model the whole tank.

Instead of setting a heat flow as a boundary input, a temperature is set at the interesting boundaries. Then, a natural convection occurs inside the tank at the edges due to the temperature difference between the heat source and the water. Finally, the input power is known by measuring the total heat flux magnitude on the boundaries where the temperature condition is set. It means that there is no control on the input heat power.

1.3 Boundaries and assumptions of the study

Knowing the method which is implemented, some assumptions are made. First, the amount of heat available is calculated based on the data only for one specific supermarket[i]. Moreover, the power shifting during a day is not taken into account, the daily average of heat power is used instead (*see Appendix B*). The COP of the heat pumps is assumed to 3 as a reference and average value.

Secondly, the use of this heat afterwards is assumed as a low temperature system for the nearby neighborhood for example but this use is not set definitely at all and many other options can be developed furthermore.

About the storage itself, it is assumed for the water tank study that the initial water temperature corresponds to the return temperature from the housing estate´s heat exchangers; this value is assumed to 20°C. The condenser is immersed inside the water and then the heat exchange occurs within the tank.

Regarding the simulations, here are the main assumptions made:

- The storage is done without any water extraction.
- Each heat source uses a Dirichlet condition, that is to say the temperature at the heat source boundaries is always maintained to *35°C (see Appendix E).*
- All around the tank shell, the Neumann condition is used by setting a heat transfer coefficient of *5,5W/(m^2.K)* because the surface resistance of the soil is assumed to 0,18 (m^2.K)/W[ii]. The soil composition and temperature are assumed homogeneous.

The problem is simplified and assumed as ideal regarding the connection from the supermarket´s refrigeration devices to the tank. Indeed, the heat bridges which can be created through the shell by this connection are not taken into account and the condenser is supposed floating and still inside the water.

In addition, the material properties and resistance of the shell of the tank are not taken into account for any of the simulations.

More detailed assumptions used for each different model cases will be developed later in the report.

To summarize the project framework, the global issue tackled can be illustrated as the one below:

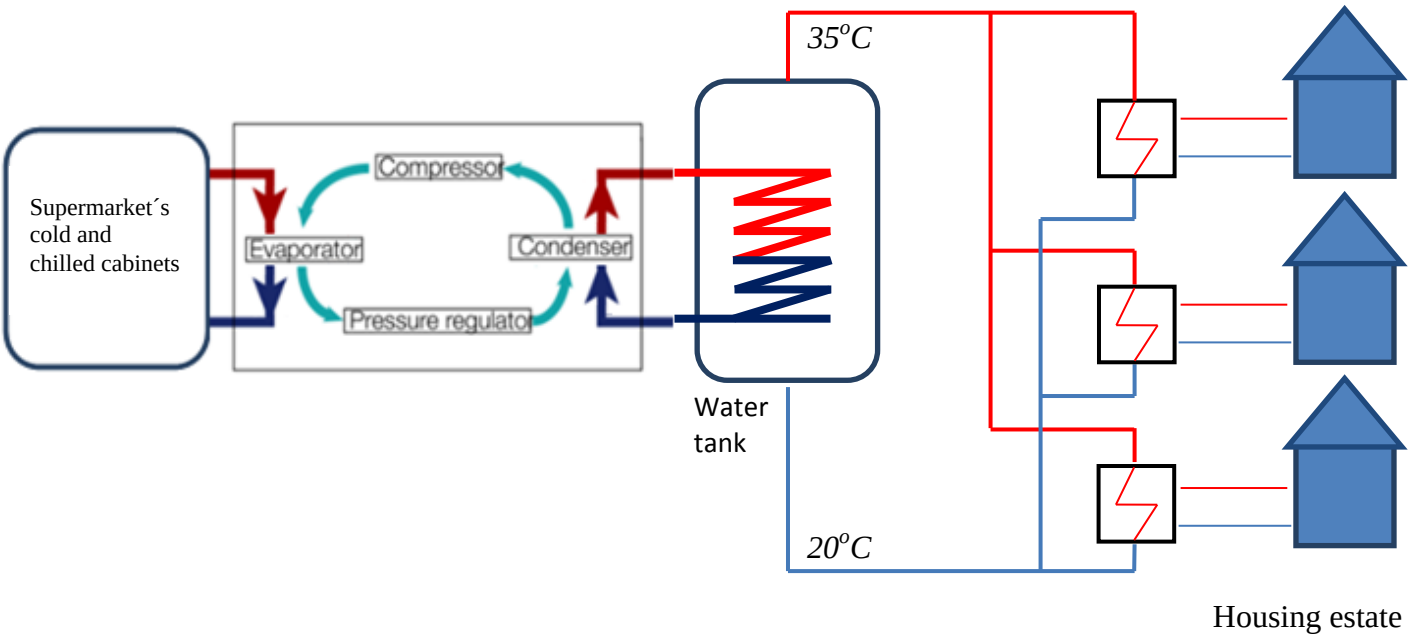

Figure 1.2: Heat network from the supermarket towards a housing estate

2. Description of the study

In this chapter, the refrigerating process is detailed and the physical and geometrical model is described together with the equations involved.

2.1 The vapor compression process

The first stage of the study is to estimate the available waste heat at the condensers. To do that, the thermodynamics refrigerating process has to be developed.

Here are the schemes of the refrigerating pump´s components and the thermodynamics cycle[iii] studied:

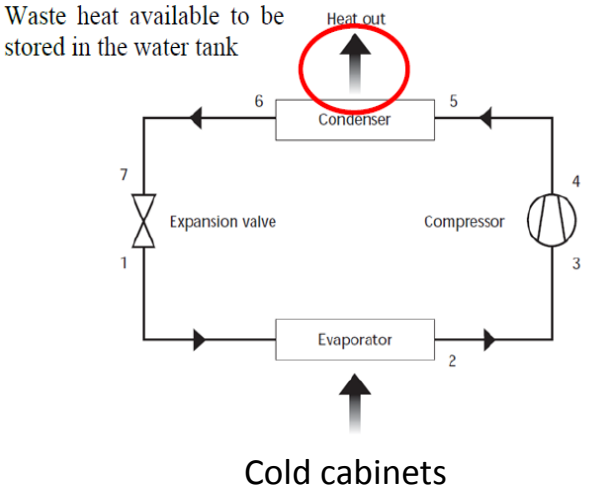

Figure 2.1: General refrigerating pump principle and components scheme

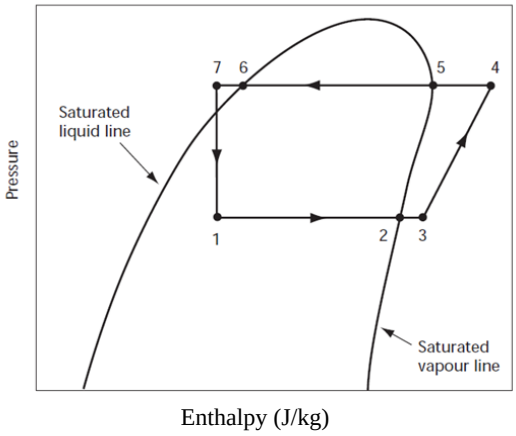

Figure 2.2: Pressure – Enthalpy thermodynamics diagram of the refrigerating pump process

At the evaporator, heat is extracted from the cold cabinets. Then, the pressure of the gas is increased in the compressor before entering the condenser where the phase changing stage occurs. The condensation releases heat towards an outside ambiance.

The amount of heat available depends on the coefficient of performance (COP) of the refrigerating pump which is directly linked to the electrical power consumed by the compressor. As this consumption has already been introduced as almost half the overall one of a typical supermarket and the COP is assumed to 3, the amount of heat available is significant.

2.2 Model properties

The following chapter develops both the thermodynamics and physical properties of the model, as well as the parameters chosen to build the geometry. Instead of running the simulations a 3D model, the study is done in 2D considering the middle section of the 3D tank in a vertical plan.

2.2.1 Water properties

Regarding the heat capacity and the thermal conductivity properties of water, their evolution over the temperature shows that they can be assimilated to constant values[iv] respectively equal to 4180 J/(kg.K) and 0.605 W/(m.K) in the temperatures range (from 10°C to 35°C) of all the studies carried out. Thus, using constant values can allow decreasing the calculation time.

However, because the buoyancy phenomenon applied to water is based on the water density difference, the parameter *rho* has to evolve according to the temperature even if the figure 2.4 below shows that the value of the density changes only of 1% in the temperature domain. The dynamic viscosity has also to vary during the simulations since its evolution over the temperature does not allow assuming it as a constant. Indeed, as shown of the figure 2.3 below, its value is divided by two between the lower and the upper temperature limits encountered in the whole study.

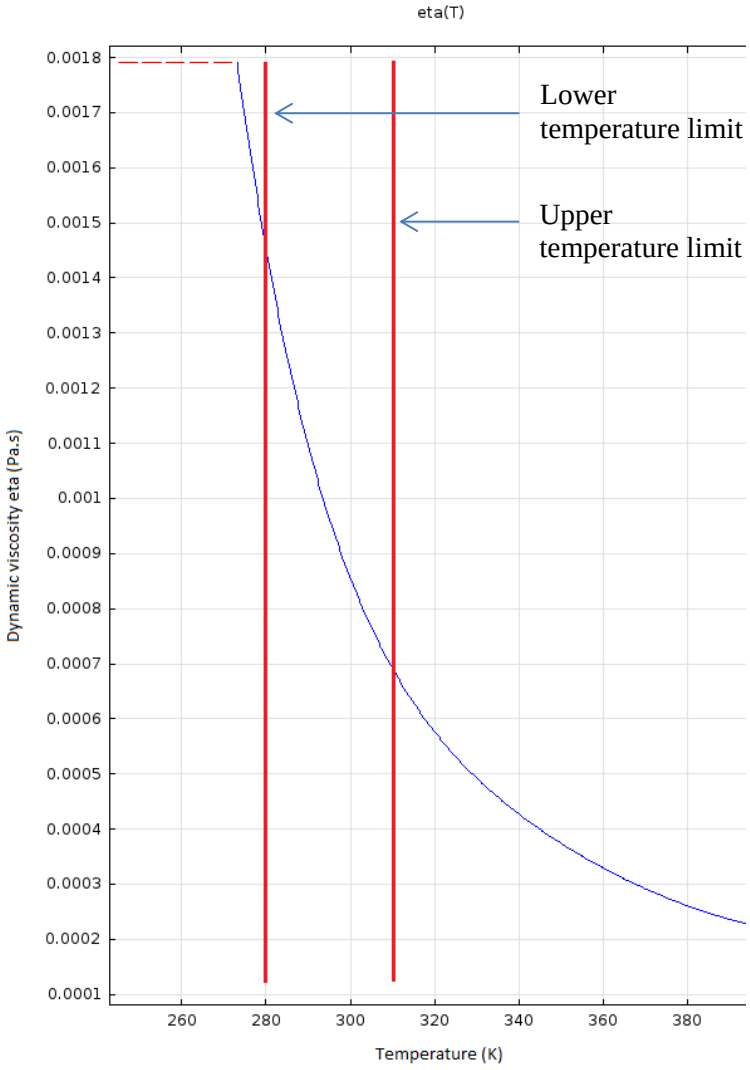

Figure 2.3: Dynamic viscosity evolution over the temperature

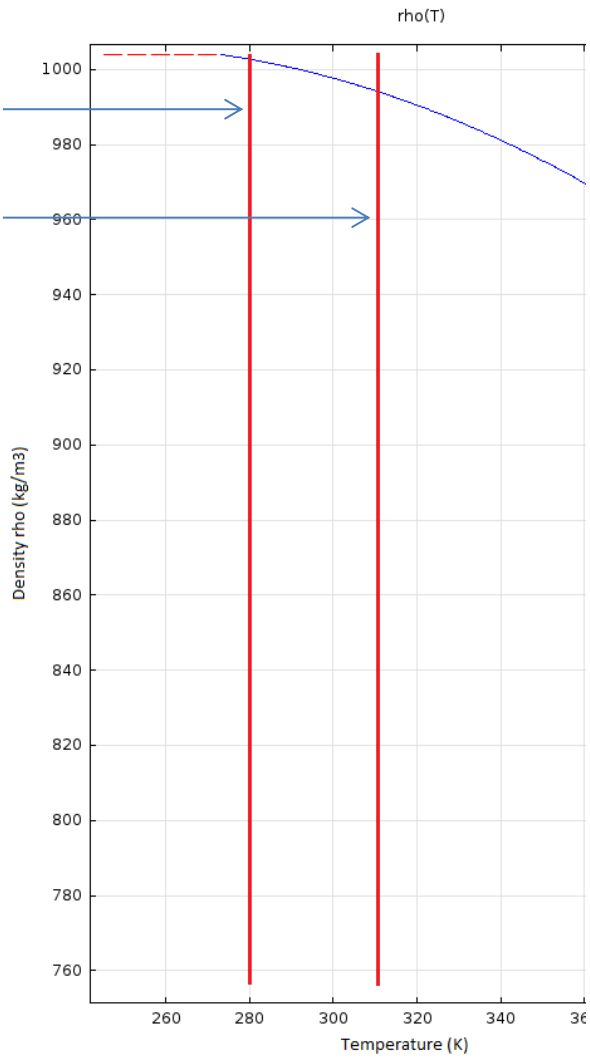

Figure 2.4: Density evolution over the temperature

A preliminary study is done on an arbitrary tank to confirm these assumptions:

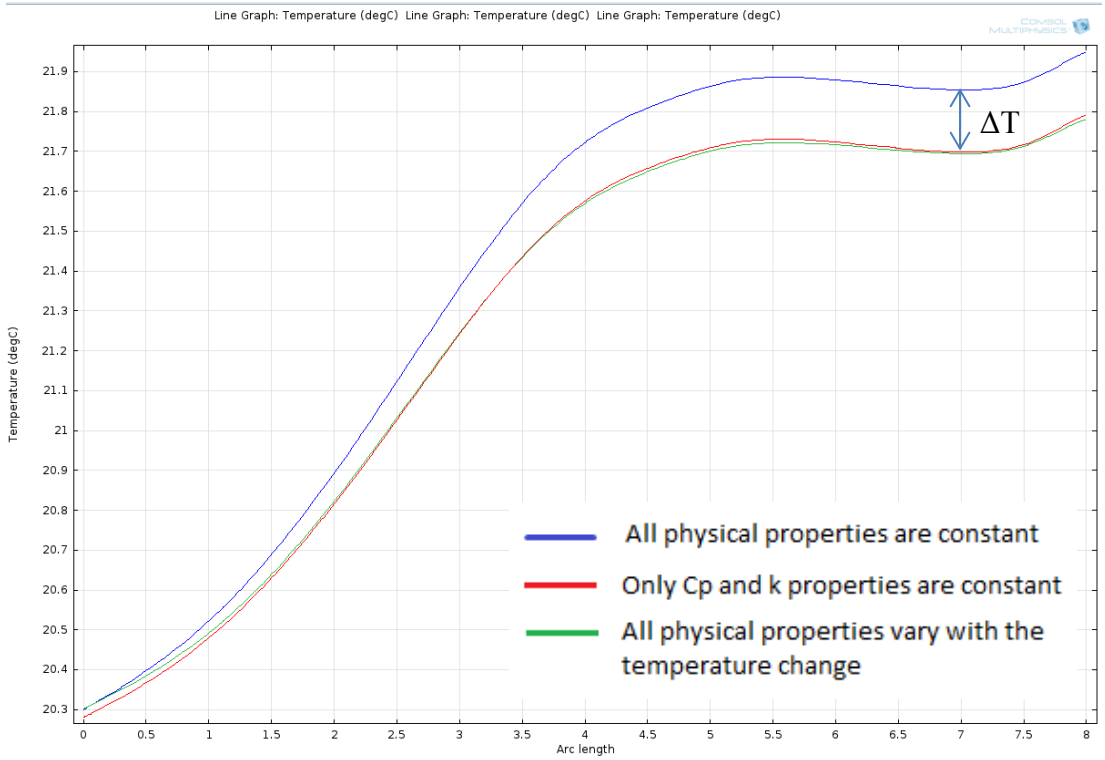

Figure 2.5: Relevance of the hypothesis of taking Cp, eta and k constant

The figure 2.5 proves that only the heat capacity and the thermal conductivity can be assumed as constant. Indeed, the results are identical when all the physical properties vary with the temperature and when only the heat capacity and the thermal conductivity are constant. Moreover, the temperature difference ΔT observed on the chart above confirms that it is not possible to consider all the parameters of water as constant since a 10% margin error appears between the accurate case and the one where these assumptions are made.

2.2.2 Parameters used

In order to be able to change easily the parameters studied using the "Parametric sweep" tool on COMSOL, all the studies carried out are parametric. Here are most of the main parameters used:

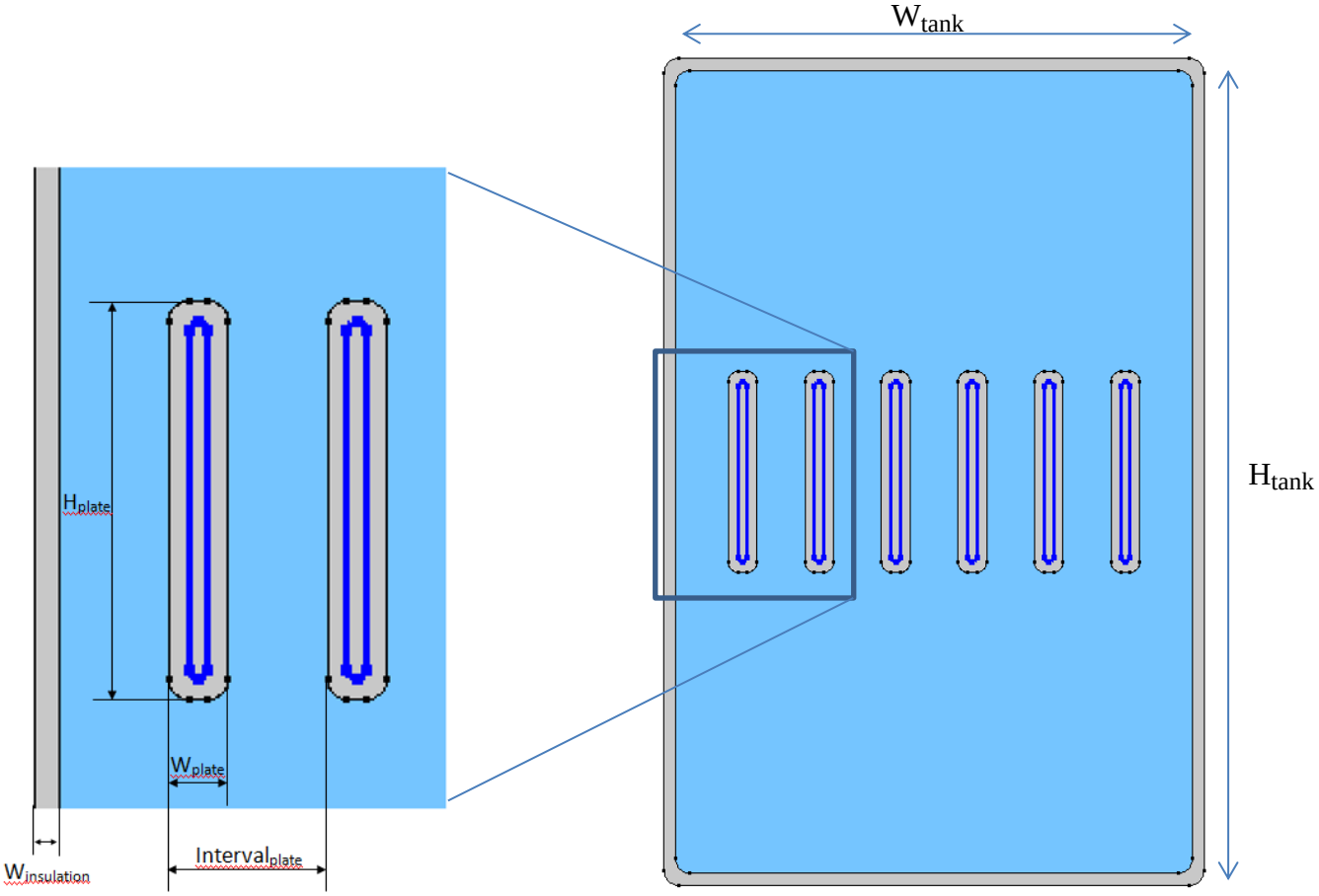

Figure 2.6: Parameters used for most of the simulations

2.3 Physical model

Before starting the simulations, it is necessary to determine the physical model that should be used on COMSOL. To this end, the type of convection and the kind of flow involved have to be determined.

2.3.1 Dimensionless numbers

Because of the heat source creating a temperature gradient within the tank, convection will appear in the tank. Forced convection occurs if[v]:

$$\frac{g * \beta * \Delta T}{U^2/L} \ll 1 \qquad (2)$$

The ratio is around 10^6 which means that the buoyancy force is high compared to the inertial force. Then, free convection will occur within the tank.

In order to determine what kind of simulation has to be run on COMSOL, it is important to determine first whether the flow will be laminar or turbulent.

The kind of flow is known by calculating the Grashof number as follows:

$$Gr = \frac{\rho^2 * g * \beta * \Delta T * L^3}{\mu^2} \quad (3)$$

The properties taken into account here are given for a temperature of 300K, which corresponds to the mean temperature used in the model.

Table 2.1: Thermo-physical properties of water at 300K[vi]

Parameters	Water at 300K
ρ	996.5 kg/m^3
β	2.76*10^{-4} K^{-1}
ΔT	15 K
U	4*10^{-4} m/s
L	8 m
μ	8.52*10^{-4} kg.m^{-1}.s^{-1}

Then, $\mathbf{Gr = 2,9 * 10^{13}} > 10^9$ which means the flow is clearly turbulent since the transition between the laminar and the turbulent flow corresponds to a Grashof number of 10^9[vii].

2.3.2 Turbulent flow model

Now this statement is done, the right flow model has to be used on COMSOL. Regarding the fluid dynamics field, the "Non-Isothermal Turbulent Flow" with the k-ε interface[viii] which combines the heat equation with the equations for turbulent flow is used for the simulations. This model allows describing the effects of the convection and the diffusion of turbulent energy, which is the case studied here. Moreover, this choice is made because this k-ε model is relevant for such a study with low pressure gradients. Indeed, as there is no inlet nor outlet in the tank, the mean pressure gradients is small and then the study remains within the k- ε model´s limits. Thus, turbulence effects are modeled using the standard k-ε model which involved the two transport equations following provided by COMSOL:

Transport equation for k:

$$\rho\frac{\partial k}{\partial t} + \rho(\mathbf{u}\cdot\nabla)k = \nabla\cdot\left[\left(\mu + \frac{\mu_T}{\sigma_k}\right)\nabla k\right] + P_k - \rho\varepsilon \quad (4)$$

The production term is written as:

$$P_k = \mu_T\left(\nabla\boldsymbol{u}.(\nabla\boldsymbol{u} + (\nabla\boldsymbol{u})^T) - \frac{2}{3}(\nabla.\boldsymbol{u})^2\right) - 2/3\rho k\nabla.\boldsymbol{u} \quad (5)$$

Transport equation for ε:

$$\rho\frac{\partial \epsilon}{\partial t} + \rho(\mathbf{u}\cdot\nabla)\epsilon = \nabla\cdot\left[\left(\mu + \frac{\mu_T}{\sigma_\epsilon}\right)\nabla\epsilon\right] + C_{\epsilon 1}\frac{\epsilon}{k}P_k - C_{\epsilon 2}\rho\frac{\epsilon^2}{k} \quad (6)$$

The two dependent variables introduced are:

- k, the turbulent kinetic energy
- ε, the dissipation rate of turbulent energy

In this model, μ_T is the turbulent dynamic viscosity such as:

$$\mu_T = \rho C_\mu \frac{k^2}{\varepsilon} \quad (7)$$

Where C_μ is a model constant on COMSOL

2.4 Model inputs

This section explains how the COMSOL model is built and which boundary conditions are used.

2.4.1 Non-slippery boundary condition

The velocity field adjacent to the interior walls at the edge with the solid insulation layer is set to be null, this is the common physical boundary condition of non-slippery walls for fluid flow. To fulfill this state in a turbulent flow model, the boundary condition on COMSOL for all the interior walls has to be set as "Wall functions". It applies wall functions to solid walls in a turbulent flow. Thus, "Wall functions" are used to model the momentum boundary layer near the wall with high gradients in the flow variables.

2.4.2 Initial values

For the transient simulations it is important to set all the initial values regarding the velocity field, the pressure and the temperature. First, the initial velocity field $\boldsymbol{u}$ is null in the water domain because the water is considered as motionless at the beginning.

The relative pressure expression within the water is:

$$P = rho * g_{const} * (H - y)\ \ [Pa] \quad (8)$$

Rho is the density [kg/m^3] of the water at the considered temperature, H represents the height of the tank [m] and g_{const} is the acceleration of gravity (a predefined physical constant in COMSOL equal to 9.8066 m/s^2). Then, the pressure is null at the top of the tank and it will increase towards the bottom.

The initial temperature is set as a parameter: T_{init} = 20°C. It means that the initial case consists of a tank totally discharged from its hot water and then filled of 20°C return water from the housing estate.

2.4.3 Volume force and pressure constraint point

In order to be able to visualize the water movements due to the difference of density according to the difference of temperature, the vertical component of a "Volume force" F is added to the water domain. It represents the gravity force applied on a volume of water such as:

$$F = -rho * g_{const} \quad [N/m^3] \tag{9}$$

Then, a pressure constraint point has to be set at the top corner to know afterwards the absolute pressure everywhere in the water. This constraint point P_o is set to 0 Pa.

2.4.4 External boundaries

Regarding the external boundaries, the shell is in contact with the ground such as T_{ground} = 10°C[ix], that is why a heat transfer coefficient has to be set in order to take into account the heat exchange through the external shell. To estimate its value, a surface resistance of 0,18 m^2.K/W is assumed. Then, it leads to h_{ground} = 5.5 $W.m^{-2}.K^{-1}$ which is applied to model the heat transfer through the ground all around the tank. This heat exchange is modeled according to the Neumann condition by adding a heat flux q_o on all the external walls such as:

$$q_0 = h_{ground}\,(T_{ground} - T\,)\ [\mathrm{W/m^2}] \tag{10}$$

Then, this flow will always be negative and represents the amount of heat lost by conduction towards the outside.

2.4.5 Heat transfer in solids

The solid domain representing the insulation layer all around the tank is assigned with the "Heat transfer in solids" on COMSOL. The heat transfer is led by the equation[x]:

$$\rho Cp\left(\frac{\partial T}{\partial t} + \boldsymbol{u}.\nabla T\right) = \nabla.(k\nabla T) + Q \tag{11}$$

However, in these solid layers does not occur any heat transport by motion and there are without any heat production. Then, the equation can be simplified by:

$$\rho Cp\left(\frac{\partial T}{\partial t}\right) = \nabla.(k\nabla T) \tag{12}$$

Thus, the conductive heat transfer through the solids is defined for all the domains concerned.

2.4.6 Heat and flow symmetry

First, the simulations are done on the whole vertical middle section tank and the results showed a symmetrical velocity profile. That is why the problem can be considered as symmetric about the vertical z axis. Thus, for this first series of simulations, only the right part of the tank is modeled on COMSOL. By adding a flow and heat symmetry line to the model, it is possible to know the velocity field and the temperature profile in the whole tank, reducing the calculation time.

The mockup of the water tank is shown below:

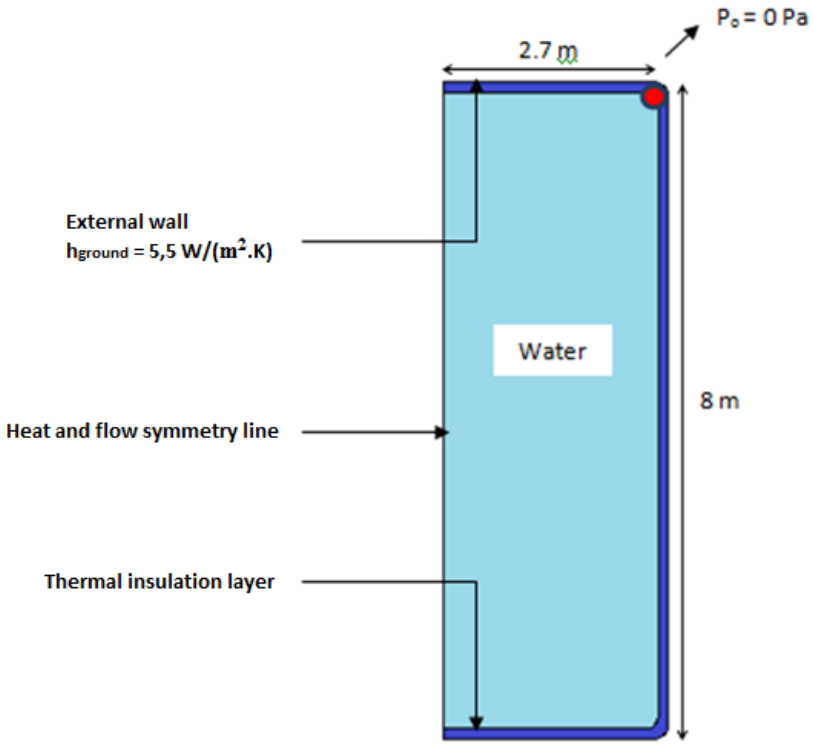

Figure 2.7: Symmetrical insulated water tank model

2.4.7 Definition of the mesh

In order to be the most accurate as possible regarding the mesh elements and to gain calculation time, the mesh must be thought beforehand. The idea is to build a coarse mesh in the middle of the tank where no high temperature and velocity gradients occur. The mesh is refined close to the sensitive domains like the boundaries where the heat source is set. Moreover, a fillet of 15 mm is built on the four corners of the tank in order to smooth these sharp angles at the corners and avoid numerical issues during the calculations.

Regarding the boundary layer all around, the mesh must be built finer on these edges where the momentum boundary layer appears and then the velocity profile is the most unsteady, meaning there are the highest velocity gradients.

2.4.8 Physics involved

A simulation is run with a heat source set on the side of the tank. The purpose is to verify with a simple case that the physics involved is correct.

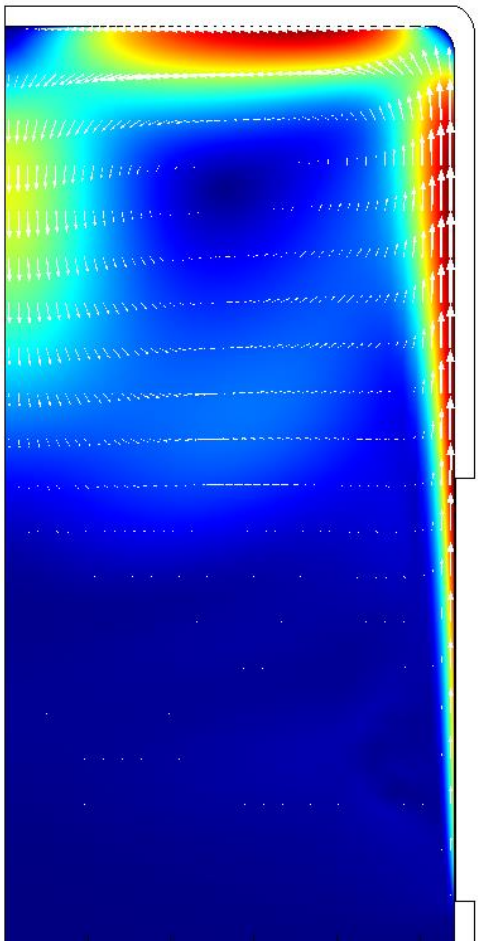

Figure 2.8: Velocity profile to visualize the free convection occurring

The velocity field on the figure 2.8 proves that the physical model is right. Indeed, when the fluid is heated up, the local density of water close to the heat source decreases, which induces an upwards flow inside the tank. The water goes along the wall and then meets an opposite flow in the middle of the tank, forcing the water to go downwards. When the velocity of the water decreases, the buoyancy force becomes predominant again. As the fluid in the lower part of the tank remains colder, the flow returns to the heat source, creating two symmetrical circular streamlines inside the tank.

3. Heat source on the edges of the water tank

The heat source is going to be added on five different locations to study the impact on the temperature distribution within the tank. The results are focused on the temperature profiles correlated to the input heat power involved.

3.1 Position of the heat source

In this study, a condition of temperature which is the parameter T_{heat} = 35°C is set on the top, the bottom and the side boundaries but also in the middle of the bottom part of the tank with two different heights (H1 and H2 that is to say respectively 1m and 2m high) as drawn below:

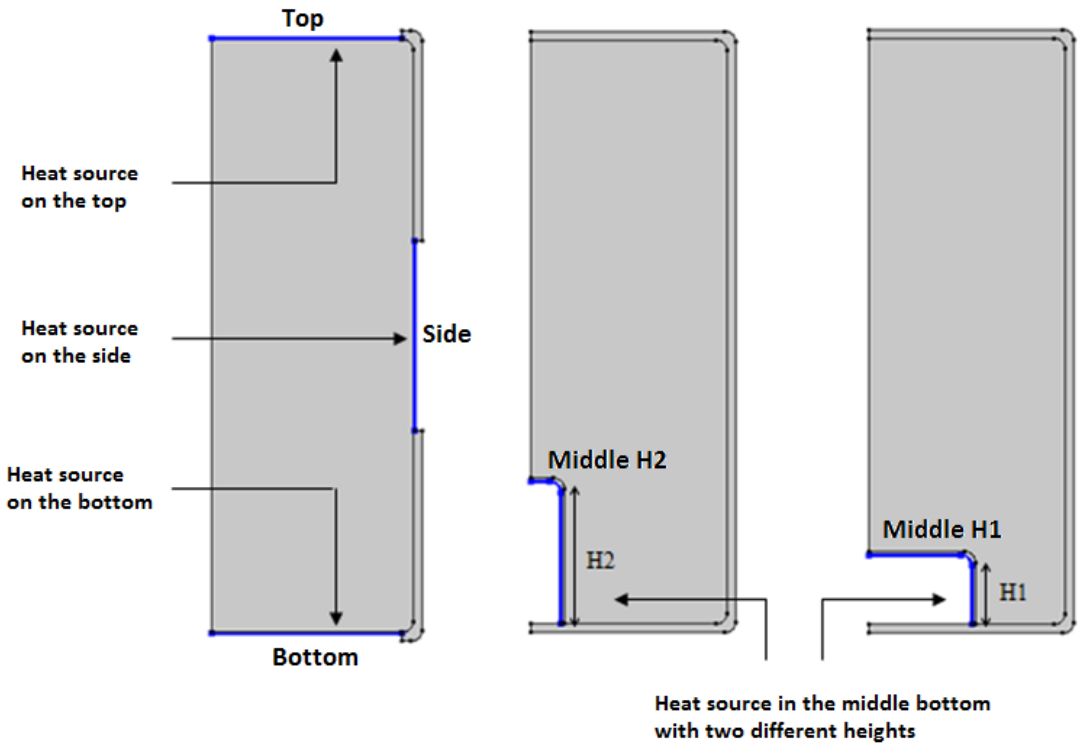

Figure 3.1: Five different locations of the heat source

Five cases will be investigated one by one and for each case, the length of the boundary where the temperature is set remains the same.

3.2 Method

The simulations are performed over a four day period (96h) to approach the steady state.

Afterwards for each simulation, horizontal cut lines are drawn each 0.5 m height to estimate the average temperature at different vertical locations.

Here is the scheme of these cut lines on COMSOL when the heat source is set on the top:

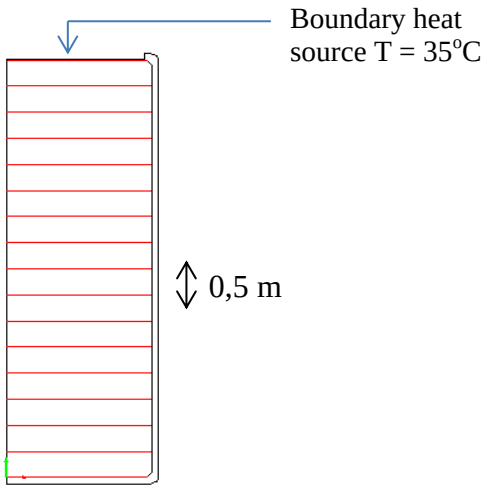

Figure 3.2: Horizontal cut lines each 0,5m step

Some additional cut lines are plotted close to the bottom and to the top parts of the tank to have more precise measurements at the edges.

3.3 Results

The temperature profiles are plotted for a time of 96h. These results are correlated with the input power evolution over the time.

3.3.1 Temperature profiles

Here are the vertical temperature profiles plotted for each case after four days:

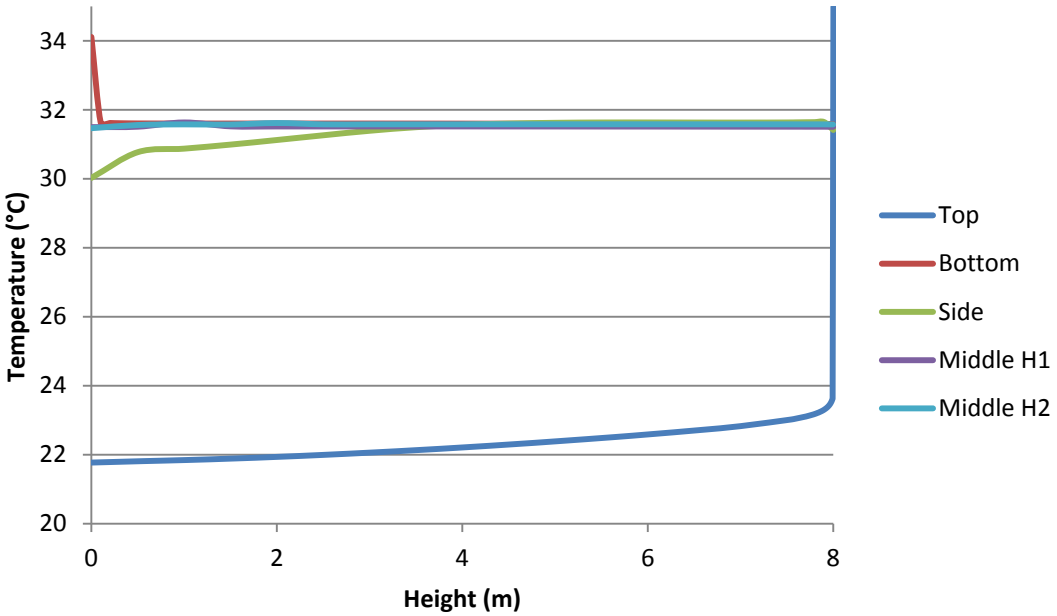

Figure 3.3: Vertical temperature profile after 96 hours

The figure 3.3 above shows that having the heat source at the bottom and in the middle leads to approximately the same results: the temperature within the tank is uniform, that is to say the stratification phenomenon all over the experiment is negligible. In addition, when the heat source is set on the middle, the height of the plates does not matter at all.

When the heat source is placed on the side of the tank, the water on the lower part is colder whereas the water on the upper part is warmed up and reaches the same temperature as in the bottom case. Thus, the stratification phenomenon is observable since there are two different layers of water in the tank: the hottest water on the top part of the tank and the coldest part remains on the bottom.

The stratification phenomenon also occurs with the case where the heat source is placed on the top of the tank. However, it can be noticed that for every time, this case leads to an overall lower average temperature of the water than in the other cases. It means that the input power in that case is low compared to the other experiments, and it can be explained by a low natural convection in the tank. Due to the heat source placed on the top, the water is warmed up there so its density decreases, which means that the water will flow upwards. However, as the water is already in the top part of the tank, it cannot go more upwards, and it cannot go downwards neither since its density is higher than the layer beneath it. So the water is barely renewed, leading to a low convection in the tank, which has for consequence a small heat exchange between the water and the heat source.

3.3.2 Input power

To understand the temperature profiles, an analysis on the input power is carried out as follows:

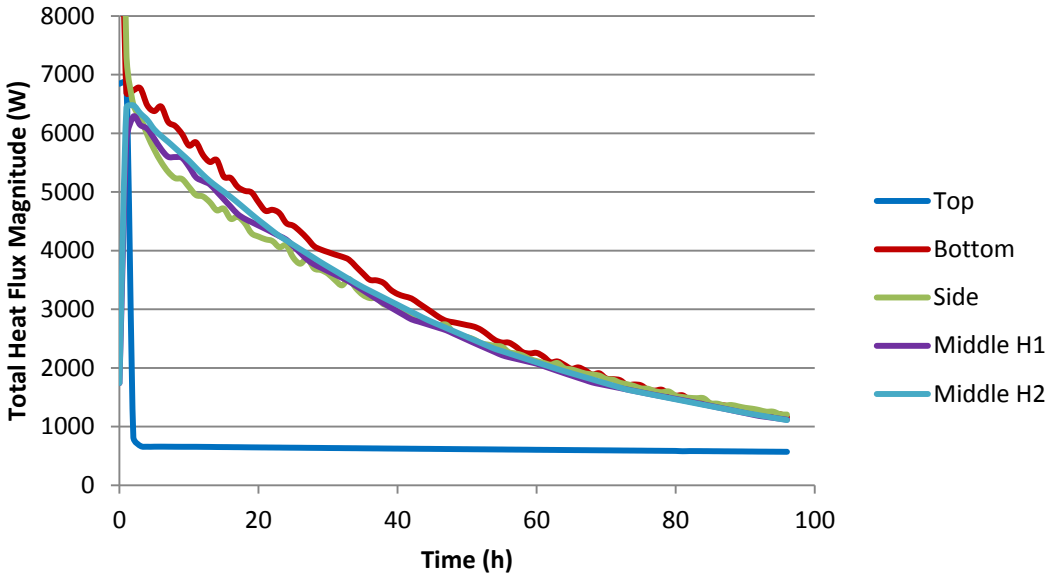

Figure 3.4: Input heat power from the temperature boundaries over the time

The figure 3.4 above displays the evolution of the input power over the time and shows that the input power is lower when the heat source is on the top part of the reservoir than for the other experiments.

The steady state corresponds to the case where the input power is equal to the heat losses through the walls of the tank. The calculations were stopped before the steady state to gain calculation time and because the evolution of the stratification phenomenon and the temperature is not important anymore after 96 hours.

This chart also shows that at the beginning of the experiment, the input power for every case is much higher than the average power during the simulation. This higher amount of power at the beginning can be explained by the initial water temperature which is set at 20°C whereas the metal plate is set at 35°C. As it heats the water up, the temperature difference decreases over the time, so the input power decreases too. It is possible to enhance the input power by increasing the temperature of the metal sheet, which will improve the natural convection within the reservoir. Another way to increase the input power is to force the convection within the tank, but mixing water will affect the stratification phenomenon. Finally, a last way to enhance the input power would be to increase the heat exchange area to improve the natural convection.

4. Heat source immersed inside the water tank

The simulations made previously gave a first overview regarding temperature distribution inside the water tank. However, these cases are still far from reality because the exchange area was limited to the edges length which cannot lead to high input powers. Once the main issue is pointed out, the idea is to increase the exchange area to foster the heat exchanges in order to increase the input power involved.

4.1 Equal space interval plates model

Regarding this issue, a second model is built where the heat source is modeled by six plates put on the top, bottom and middle of the tank. These models allow getting closer to reality where the coil is directly immersed in the water.

The purpose here is not to compare this case with the previous one because the length covered by the heat source on the edges is too short to be transposed to this new model.

4.1.1 Definition of the model

Then, six plates are implemented to increase the exchange area. Because it is hard to reach convergence on COMSOL with a symmetrical model, it is chosen to carry out these simulations on the whole section. The plates have the same interval in between each other and the same dimensions as drawn below:

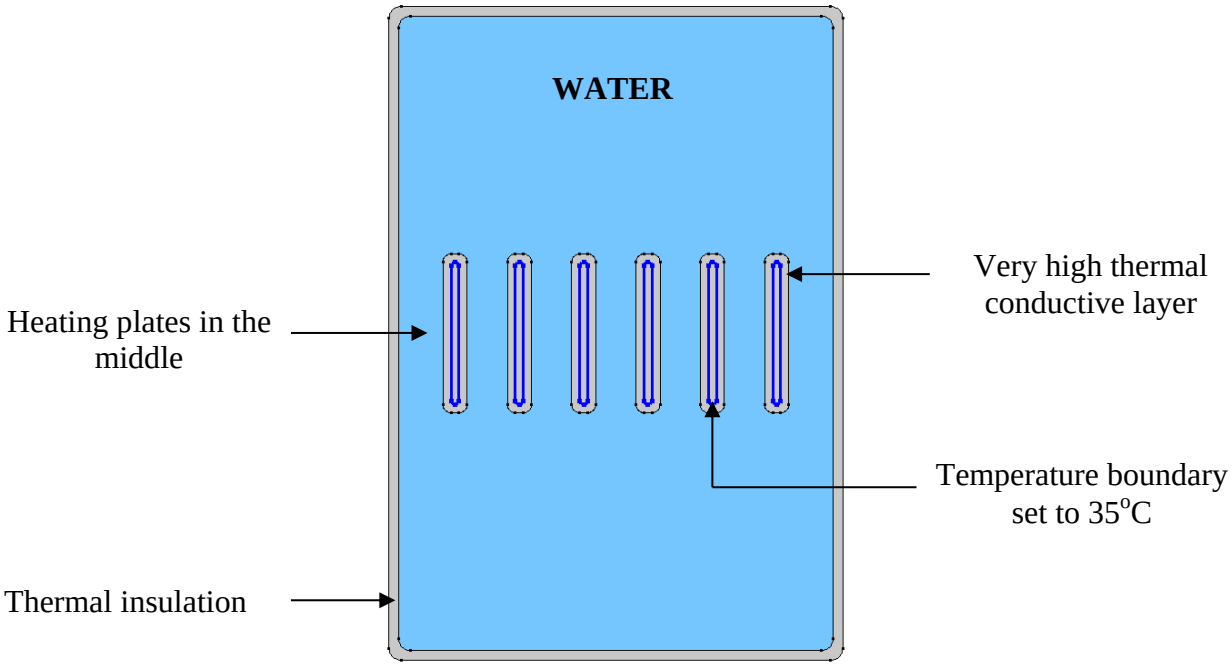

Figure 4.1: Model with immersed heating plates in the middle

These plates are also set on the top and the bottom of the tank in order to study the influence of the heat source location, as shown respectively on figure 4.2 and figure 4.3 below:

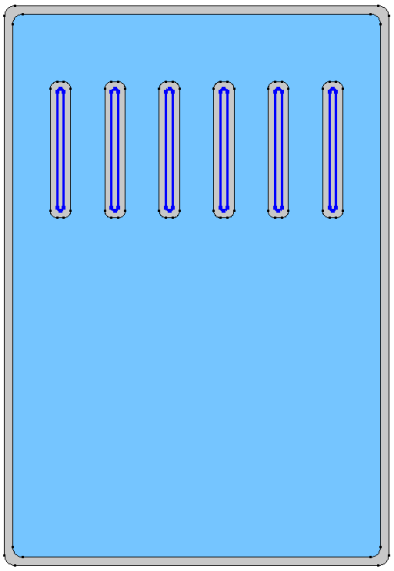

Figure 4.2: Model with immersed heating plates on the top

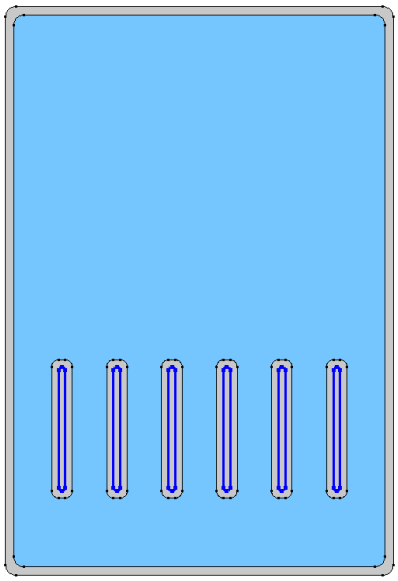

Figure 4.3: Model with immersed heating plates on the bottom

4.1.2 Method

The transient simulations are run over 48h instead of 96h since it appears that the final temperature is almost reached after two days. To exploit these results, horizontal cut lines are plotted from the bottom to the top of the tank each 0,5m step.

4.1.3 Results

The temperature profiles are plotted for two different times: after 24h and 48h. These results are also correlated with the input power evolution over the time.

4.1.3.1 Temperature profiles

Plotting the temperature profile for 5h on the figure 4.4 below only allows to see the behavior early when the simulation starts. Then, it is possible to see how fast the process at the beginning is.

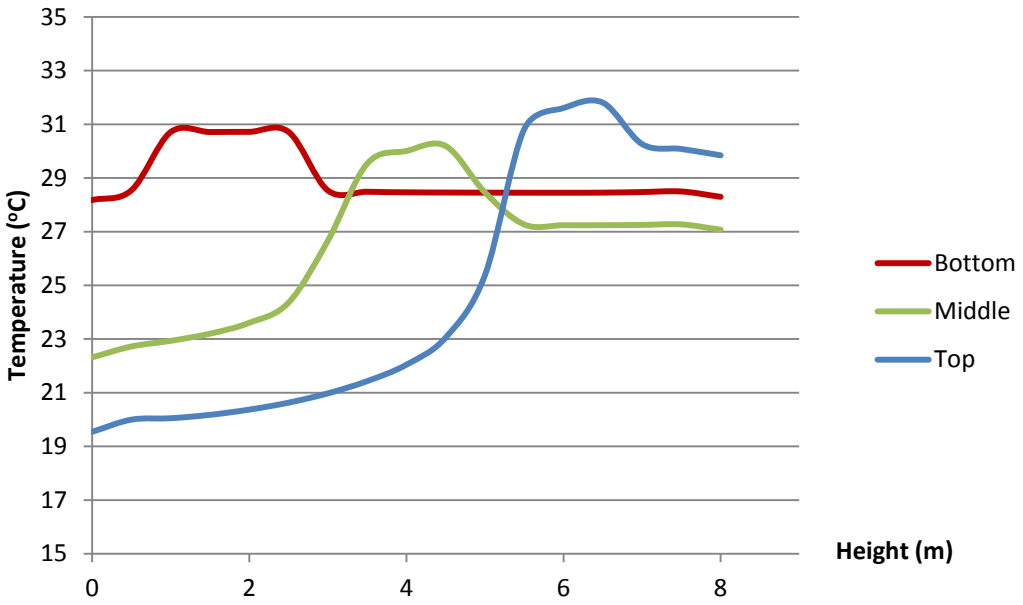

Figure 4.4: Vertical temperature profile for the 3 different locations after 5 hours

When the exchange starts, the case with the plates on the top reaches the highest temperature on the top part of the tank whereas this temperature is the lowest in the middle case. Moreover, the temperature reached for the top case is the highest whereas the middle situation leads to the lowest temperature on the top part of the tank. However, when the plates are set on the bottom, the temperature on the top remains higher than when plates are on the middle.

These first results show that the heat source on the bottom must deliver much more power than the two other cases since the average temperature is higher in the whole tank.

Here are the vertical temperature profiles plotted after one day and two days:

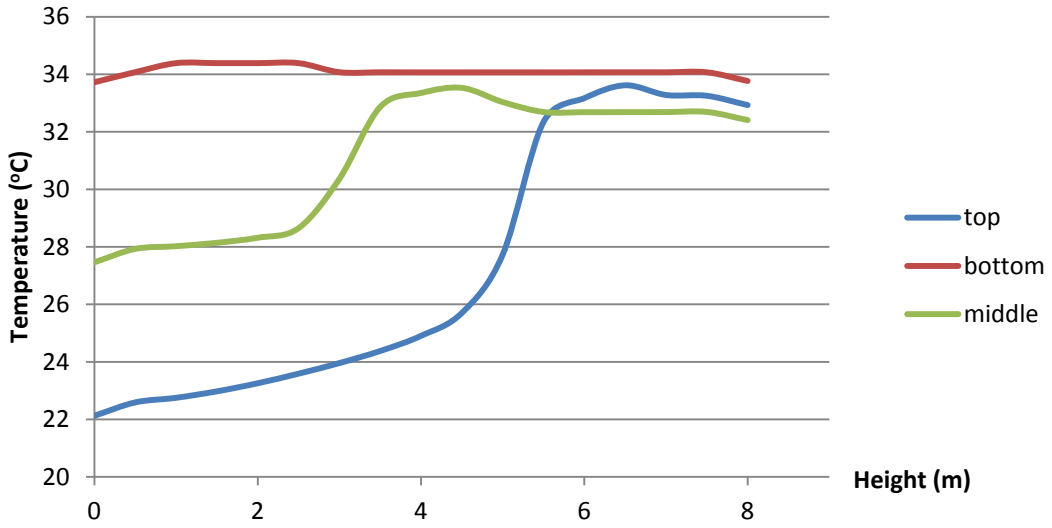

Figure 4.5: Vertical temperature profile for the 3 different locations after 24 hours

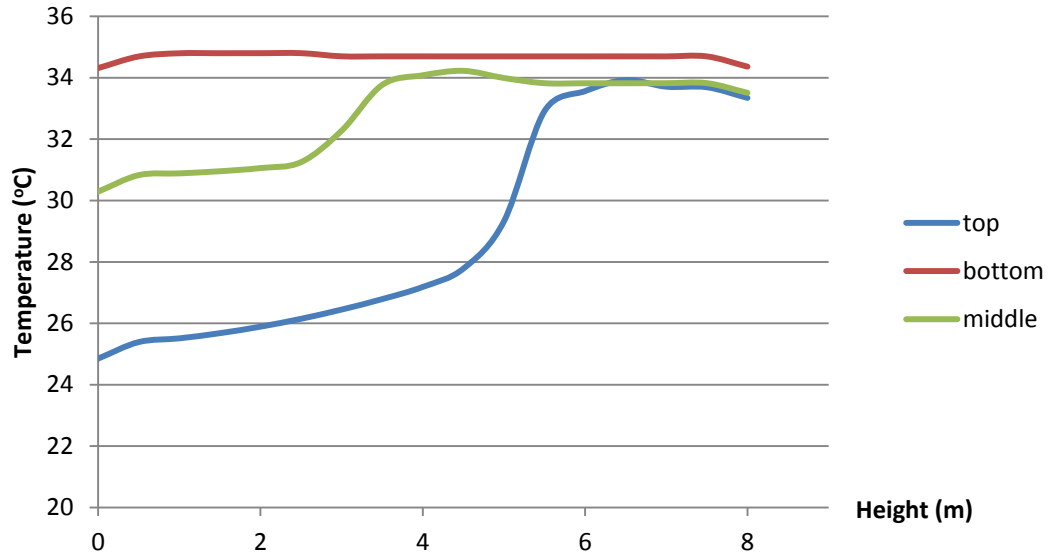

Figure 4.6: Vertical temperature profile for the 3 different locations after 48 hours

The case where the plates are set on the bottom leads to the fastest temperature rise and homogenization in the whole tank whereas the cases on the top and the middle show two distinct temperatures zones, a warmer on the top and a cooler on the bottom part. This means that a temperature gradient occurs from the bottom towards the top.

The cooler part seems to persist until higher in the tank when the heat source plates are set on the top. Then, the height of the hot layer remains smaller which means the amount of hot water available is less important than in the others cases. In addition,

from a day to another, the temperature only rises below the plates and remains unchanged on the top part of the tank.

An almost perfect symmetry seems to occur with the source in the middle, that is to say there are two temperature layers clearly separated in the tank. The warmest layer on the top is larger so this case allows having more hot water on the top of the tank than with a coil set on the top.

Putting the hot plates in the middle of the tank seems to allow having a larger amount of hot water available after two days with a clearly vertical stratification between the bottom and the top. Nevertheless, having the source on the bottom allows having faster than the other cases the whole tank heated up to 35°C.

4.1.3.2 Input power

The chart below provides information about the input power involved which can explained the temperature profiles got previously:

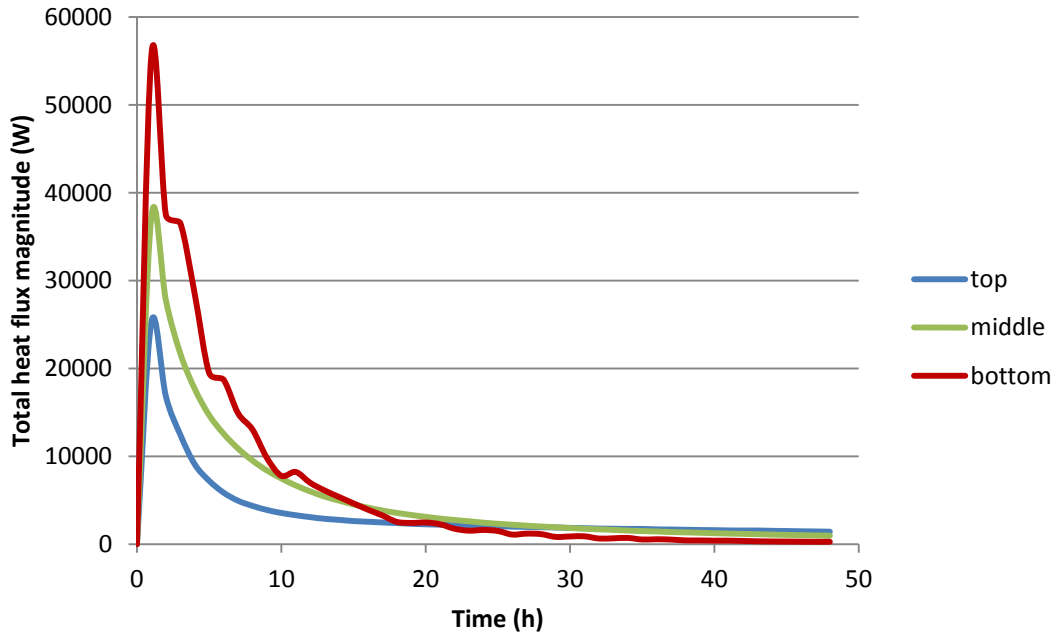

Figure 4.7: Input heat power released from the plates over the time

First, it could be noted that from the bottom to the top cases, the initial input power always drops by almost 30% between each case. The figure 4.7 explains why the temperature is always higher everywhere within the tank when the heat source is set on the bottom. Indeed, the initial input power is by far the highest and remains a little bit higher than the other ones until around 20h of simulation time. This means that a higher convection occurs, which brings a better exchange and then explains why it is easier and faster to reach a uniform temperature in the whole tank.

On the other hand, the heat source on the top provides the lowest power over the time due to a low convection quality. That is why, in this situation the water remains the coldest in the whole part below the plates and only the temperature on the top part near the sources is always kept hot.

4.2 Model of remote plates

The six exact same plates are set in a different way inside the tank. They are divided into two parts, the space interval between them has decreased and a larger space remains between these two parts. The heat exchange area remains exactly the same as previously but the simulations are now run when plates are set only on the top.

4.2.1 Definition of the model

The idea is to know how the layout of the heat source can influence the temperature distribution within the tank.

Here is the scheme of the new layout:

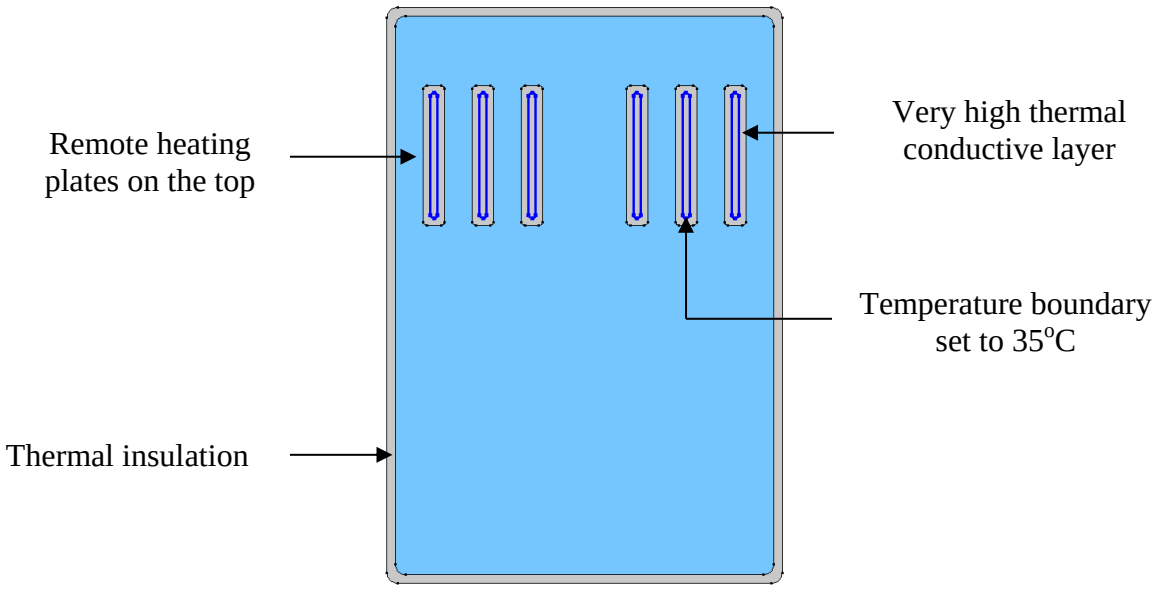

Figure 4.8: Model with immersed remote plates on the top

4.2.2 Results

To be able to compare the two models the results are plotted in parallel with the previous case when the plates are on the top:

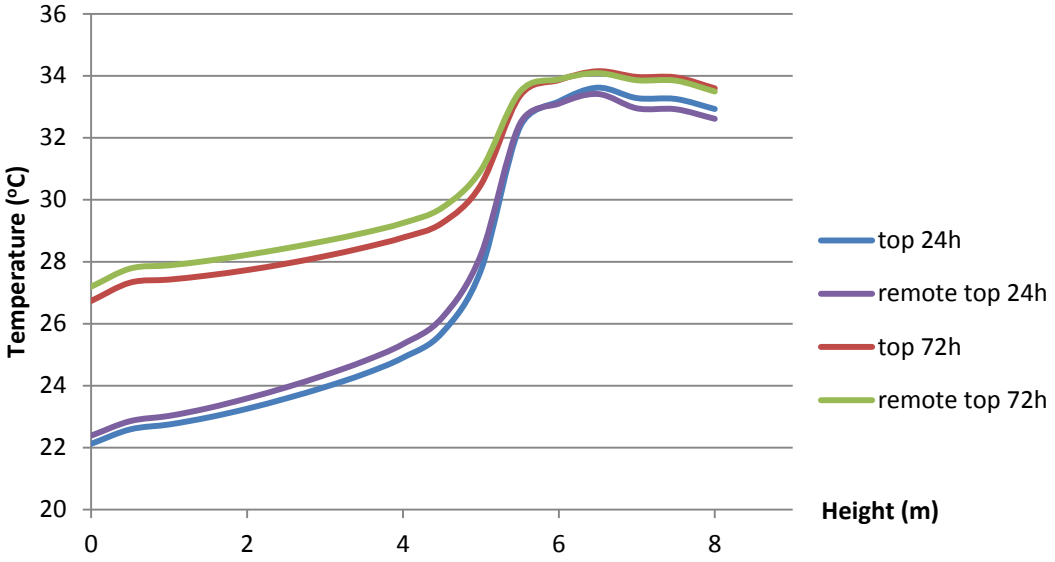

Figure 4.9: Temperature profile comparison between equal space interval and remote plates´ layout on the top

When comparing the temperature profiles on the figure 4.9 above, the values with the remote plates on the bottom of the tank are slightly higher whereas the temperature reached on the top is a little bit lower. These differences remain clearly insignificant which means that the layout does not affect the temperature reached, at all.

Having these results for the top situation and knowing that the input power is exactly the same prevents from going further, trying the other configurations.

The change can be noticed on the velocity field plotted below for the last time (72h):

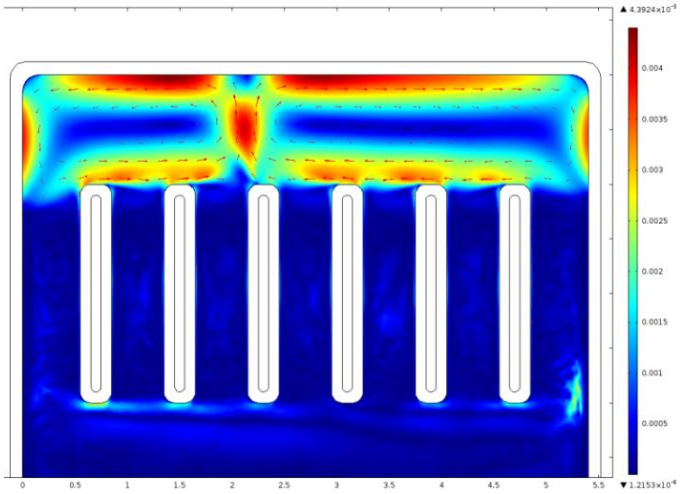

Figure 4.10: Velocity field above the equal space interval plates after 72h

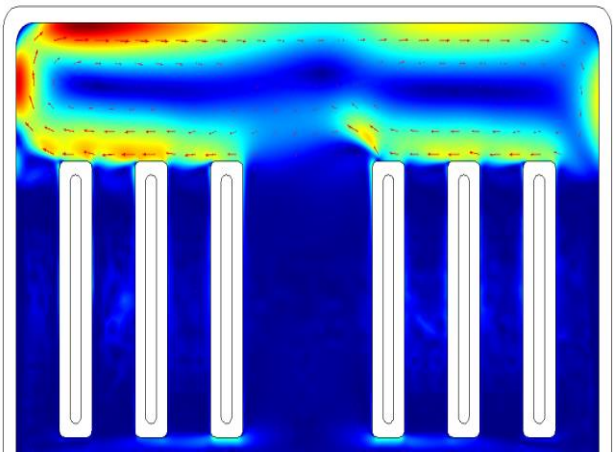

Figure 4.11: Velocity field above the remote plates after 72h

The velocity scale of the two figures above is the same, so the speed is higher on the top of the plates in the equal space interval configuration and an upward movement occurs in the middle, above the plates. This phenomenon does not appear with remote plates. Then, the exchange seems slightly lowered above the plates when these ones are remote, which can explain why the temperature reached on the top is slightly lower. Indeed, due to the gap between the plates in the remote plates´ configuration, the water flow goes downwards since there is no heat source at this specific place. Then, having a gap breaks the water movement and prevents any upwards flow.

5. Influence of the height of the tank on the vertical stratification

The influence of the height of the tank on the vertical temperature stratification is studied in this chapter.

To this end, the next simulations are done on a tank with three plates immersed in the middle of the tank. The models are made in 2D and also later on a 2D axi-symmetrical geometry.

5.1 2D model

The first simulation is made with a 2D model in order to visualize the temperature profiles in the middle section of the tank in a vertical plan.

5.1.1 Choice of the cut lines

Before comparing different temperature profiles, the location of the cut lines has to be decided in order to get relevant measurements. It is interesting to investigate what happens close to the heating plates and far from them.

First of all, it is necessary to check if the problem is exactly symmetrical. To do that, the difference of results when drawing a cut line between the two plates on the left and a cut line between the two plates on the right is shown below:

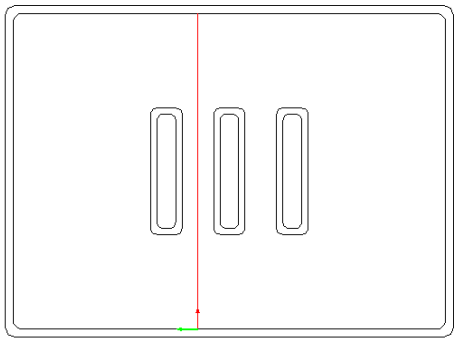

Figure 5.1: Cutline plotted between the left plates

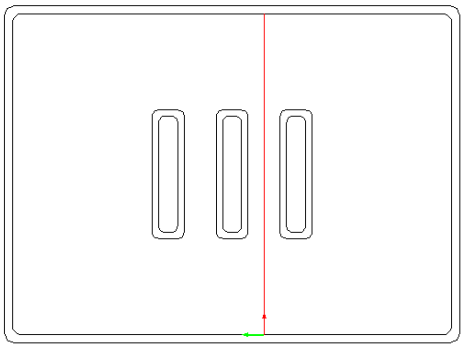

Figure 5.2: Cutline plotted between the right plates

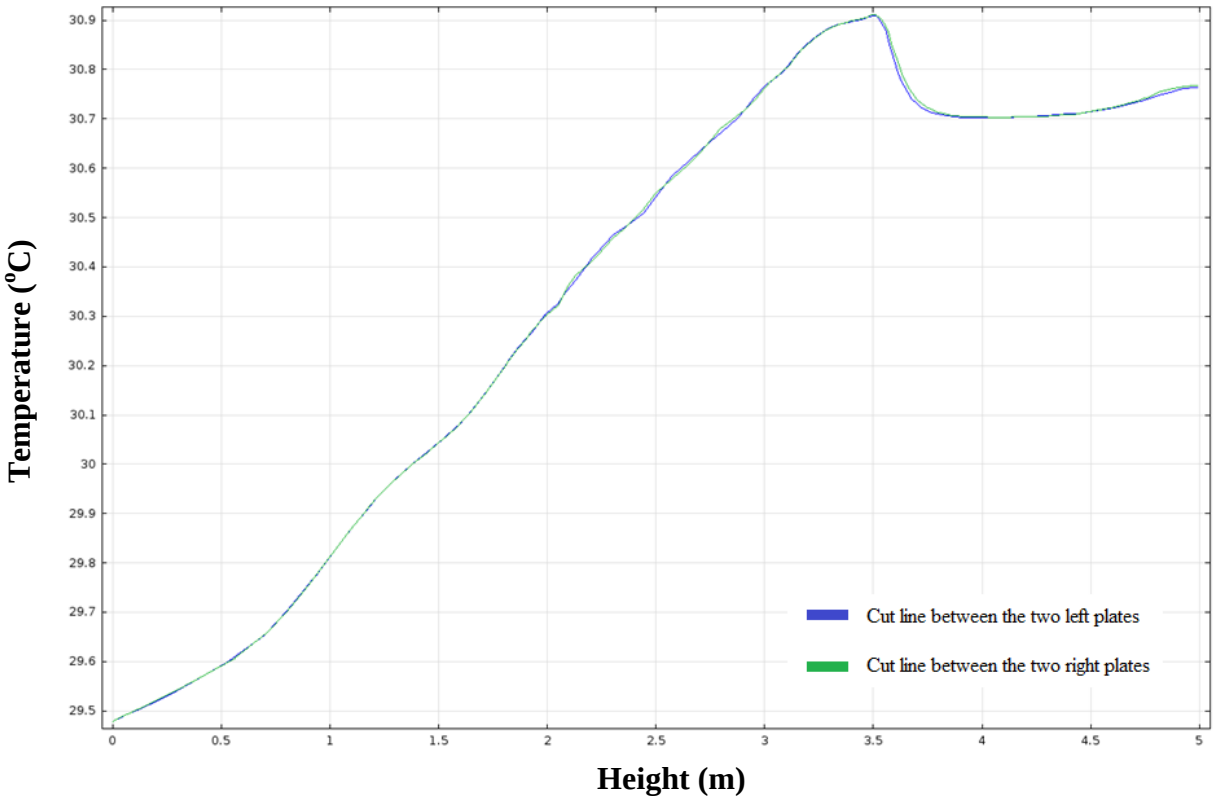

Figure 5.3: Comparison of the temperature profiles for the two configurations

The figure 5.3 above shows that there is no difference in the temperature profile over these two cut lines, which means the behavior in the water is symmetrical. Only one of them is sufficient to have a precise enough estimation of the temperature profile in this region.

The following drawings show where the temperature profiles will be measured:

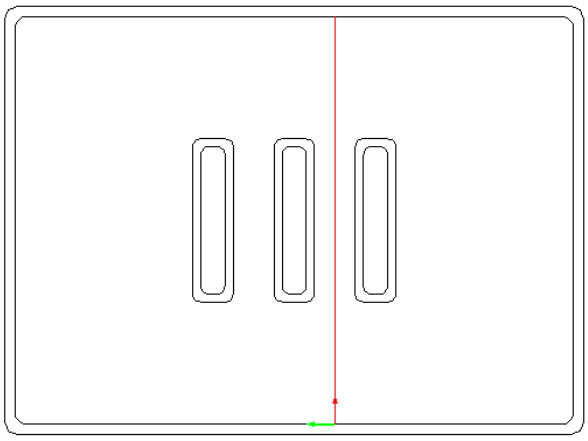

Figure 5.4: Cutline plotted at the vicinity of the plates

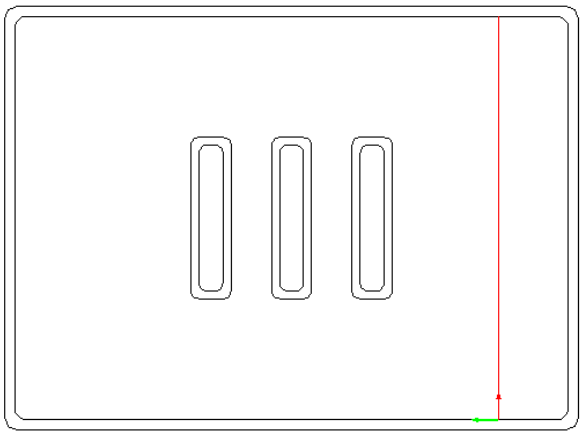

Figure 5.5: Cutline plotted away from the plates

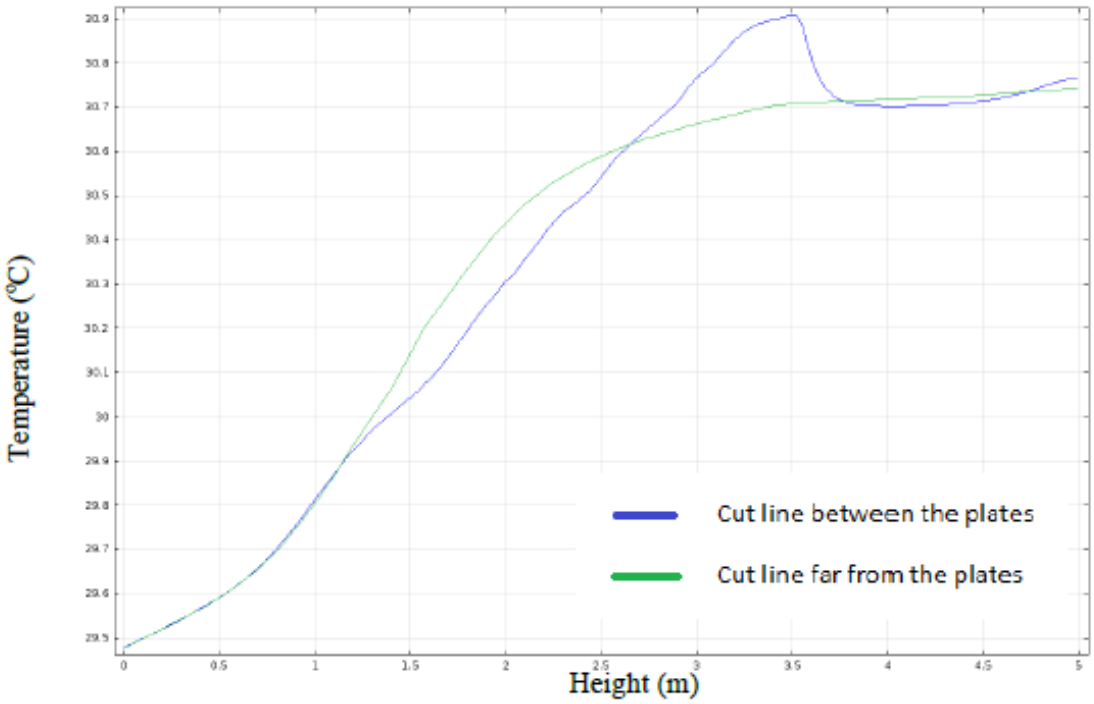

Figure 5.6: Comparison of vertical temperature profiles for these two cut lines configurations

The figure 5.6 above shows that the vertical temperature profile is not the same depending on the location where the measure is taken. A peak temperature is seen on the blue curve at a height of 3.5m which corresponds to the upper tip of the heating devices and is explained by the fact that the cut line is drawn close to them. It explains why at the tip of the plates the temperature is higher than far from them. Then, for higher heights within the tank, the temperature decreases.

5.1.2 Temperature profiles

Here is a comparison of the temperature profiles for each tank three days after the beginning of the simulation when cut lines are away from the plates:

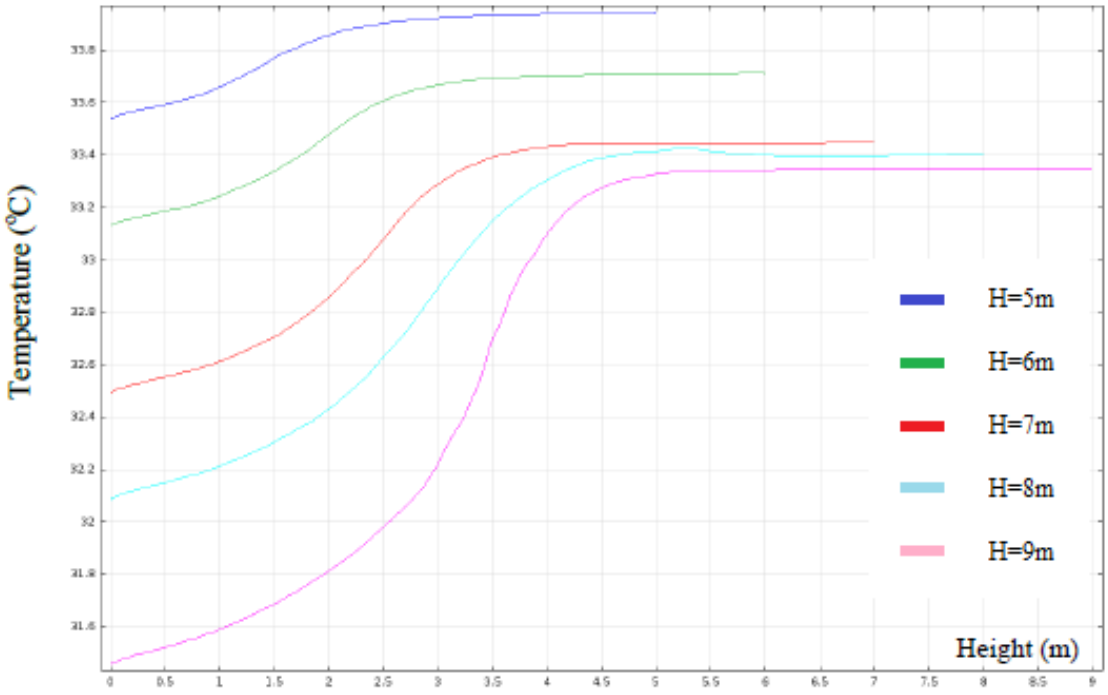

Figure 5.7: Temperature profile away from the plates after 72 hours

The figure 5.7 clearly proves that the smaller the tank is, the higher the average temperature within the tank is. The ratio in the table 5.1 between the volume of the tank and the area of the section remains even according to the difference heights. However, when calculating the ratio between the area and the perimeter of the section, the case where H=5m has the lowest ratio. It means that for the same area, the perimeter of this tank is higher than the other cases. Then, the heat losses towards the ground through the walls are higher for this 5m high tank, which should lead to a lower temperature. However, it is not what can be observed on the figure 5.7 since the smallest tank presents the highest temperature.

The density power is investigated in the table 5.1 and it appears that the input power is not as even as assumed. Indeed, the average density power is the highest for the smallest tank and keeps decreasing when the tank height increases. It can be explained by the fact that the volume of the tank is not exactly the same for all the cases. Indeed, because COMSOL considers objects with 1 meter-depth when building a 2D model, the transposition from the section to the volume is not the same in all the situations. The following equation is used to calculate the width of the section for a cylinder depending on the height:

$$width = 2 * \sqrt{\frac{volume}{\pi * height}}$$

However, since the depth of a section in COMSOL is equal to 1 m, the model does not correspond to a cylinder and the volume from one model to another is different, leading to different density powers.

Table 5.1: Ratios and density powers of the model according to the height

	Case 1 : H = 5m	Case 2 : H = 6m	Case 3 : H = 7m	Case 4 : H = 8m	Case 5 : H = 9m
COMSOL volumes (m^3)	34,3	37,6	40,6	43,4	46
Average density power (W/m^3)	205,5	203,6	197,6	191,7	183,3
Ratio (m) Area/Perimeter	1,45	1,53	1,59	1,62	1,63
Ratio (m) Volume/Area	0,37	0,38	0,38	0,38	0,38

Consequently, these results are obtained because of the density power changes from a tank to another, making impossible a comparison between the different cases. Thus, a new model using an axi-symmetry line is used for the next study.

5.2 2D axi-symmetrical model

The same simulations are run with an axi-symmetric model in order to compare it with the previous simulations. Here is the COMSOL model:

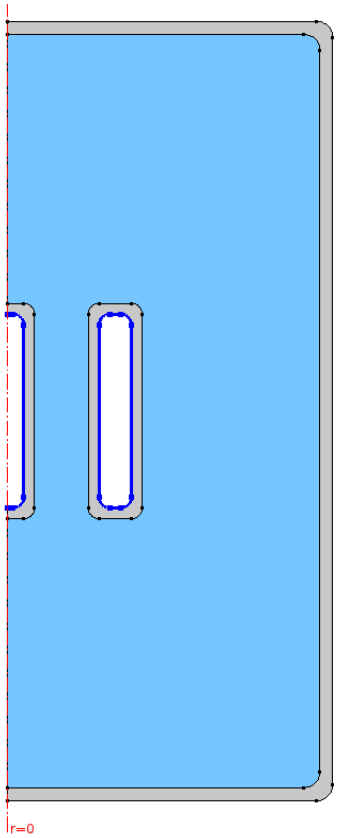

Figure 5.8: Model used for the axi-symmetry study

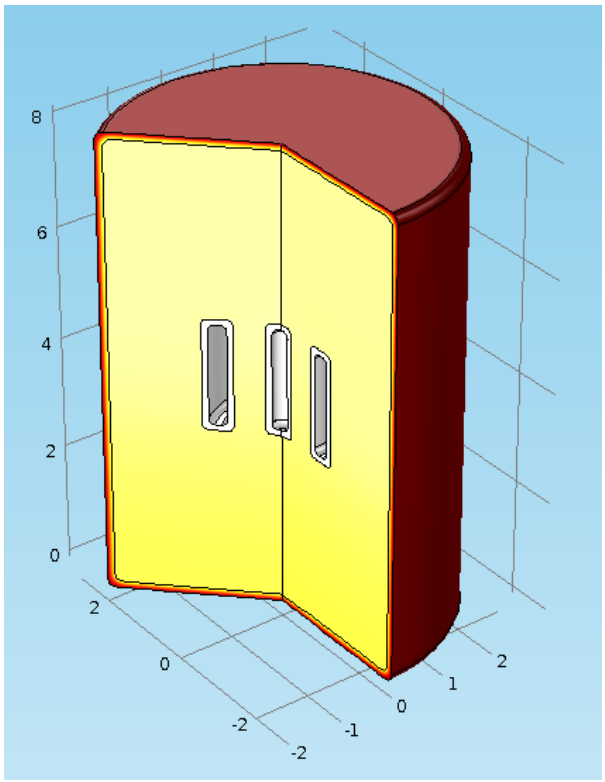

Figure 5.9: 3D model resulting from the axi-symmetry study

The figure 5.8 shows a section of the tank including the axi-symmetry line which is used to model the whole reservoir on COMSOL.

5.2.1 Choice of the cut lines

The cut lines are placed between the plates and far from them in order to evaluate the temperature profile in two distinct locations, i.e. one in the center area of the tank, close to the heating plates, and the other one in the side area of the tank, far from the heating devices as drawn below:

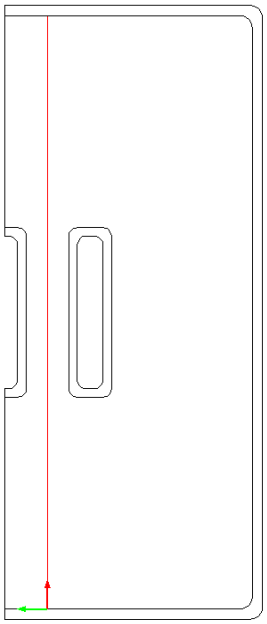

Figure 5.10: Vertical cutline at the vicinity of the plates

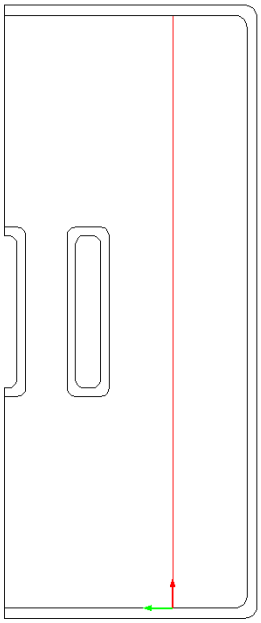

Figure 5.11: Vertical cutline away from the plates

5.2.2 Temperature profiles

The charts below draw a comparison of the temperature profiles for each tank 24 hours after the beginning of the simulation when cut lines are far from the heating devices.

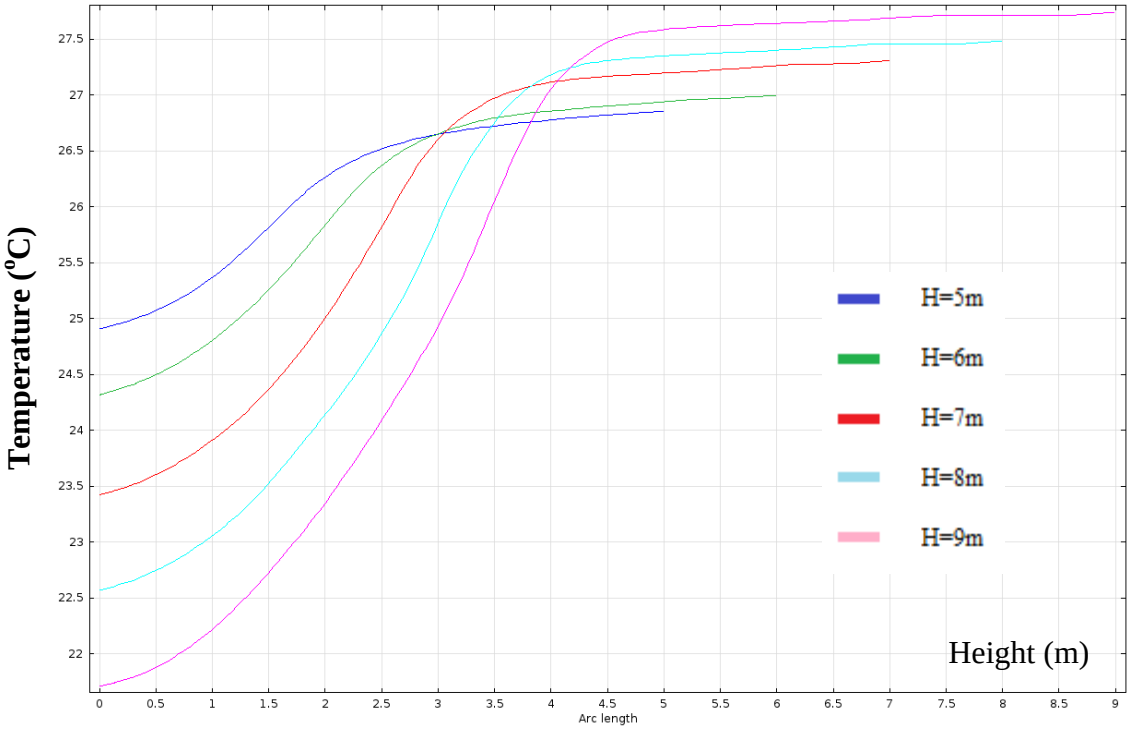

Figure 5.12: Temperature profile away from the plates after 24 hours

The figure 5.12 clearly shows that the vertical stratification within the different water tanks depends on the height of the reservoirs since the temperature difference between the top and the bottom of the tank is larger when the height increases. The temperature gradient also proves that the stratification phenomenon is more marked when the tank is higher than wide. The temperature profile is more even in small tanks than in high ones, which confirms that the vertical stratification is more pronounced in high tanks.

The figure 5.13 below illustrates the temperature profile evolution over one day for the 5m and the 9m high tanks.

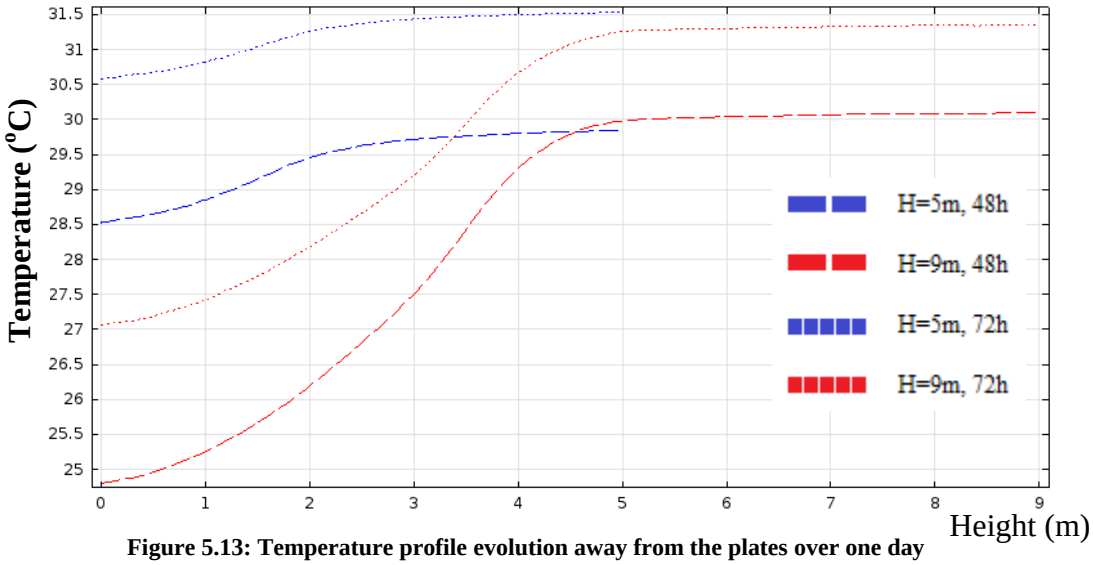

Figure 5.13: Temperature profile evolution away from the plates over one day

Once again, the figure 5.13 proves that the stratification is more important in high tanks, or in other words that the temperature distribution is more uniform in small ones. Compared to the figure 5.12, it can be observed than the temperature at the top of the 5m and the 9m high tanks is approximately the same, which is not the case 24h after the beginning of the simulation. Moreover, the temperature difference between the bottom parts of the both tanks does not change. Thus, it can be stated that the input power is more important for small tanks since the average temperature increases faster in small reservoirs.

Table 5.2: Temperature on the top and at the bottom of the tank for each height studied

	t = 24 hours	t = 48 hours	Evolution rate of the temperature from 24h to 48h
Temperature on the top when H = 9m	27.75°C	30.20°C	8.8 %
Temperature on the top when H = 5m	26.75°C	29.80°C	11.4 %
Temperature at the bottom when H = 9m	21.75°C	24.75°C	13.8 %
Temperature at the bottom when H = 9m	25.00°C	28.5°C	14.0 %

As shown in table 5.2, the evolution of the temperature at the top of the small tank is faster than the one at the top of the high tank, whereas the evolution of the temperature at the bottom of these tanks is in the same range. It means that at the very beginning of the simulation, the temperature at the top of high tanks increases quickly since it is warm faster in the upper part.

The temperature profile on the vertical cutline near the plates is now studied and the results are plotted below:

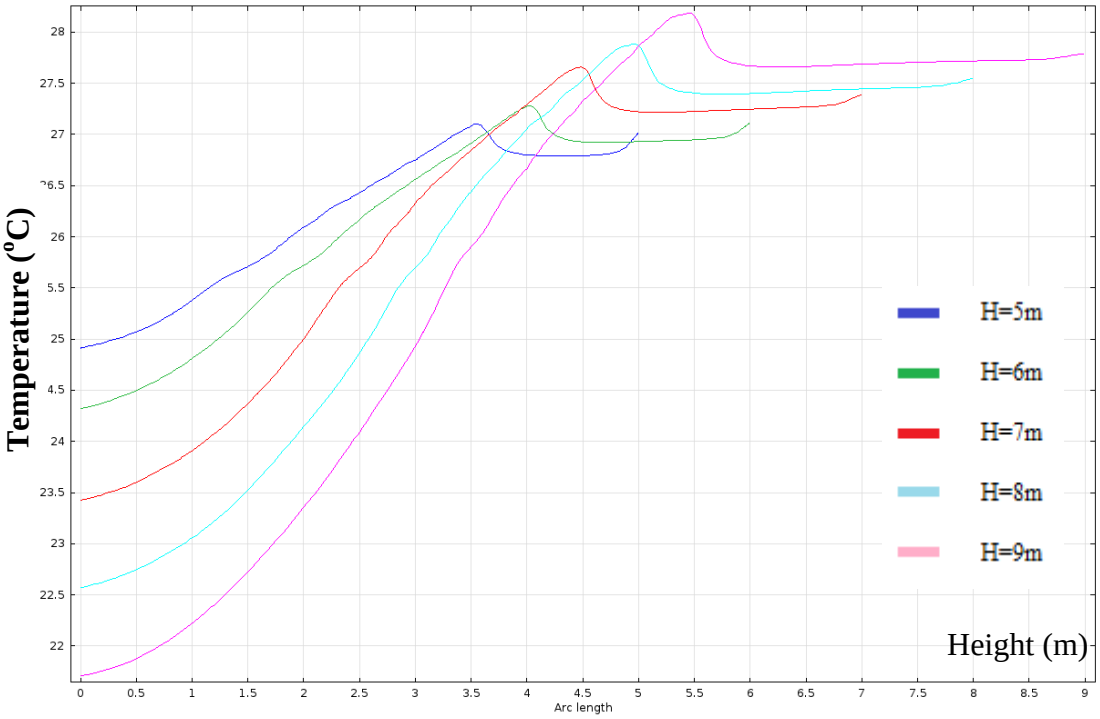

Figure 5.14: Temperature profile close to the plates after 24 hours

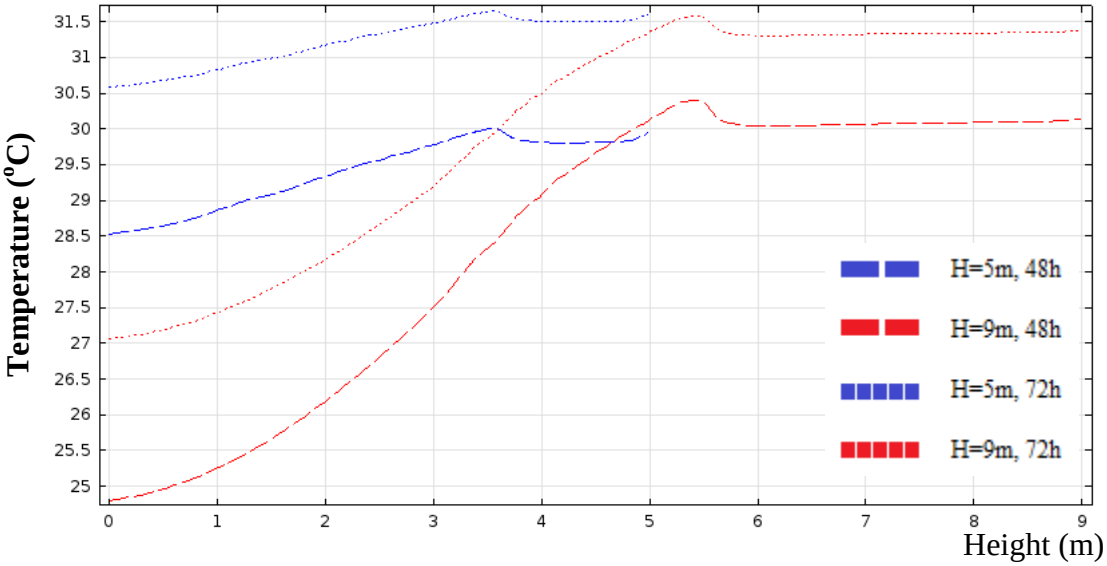

Figure 5.15: Temperature profile evolution close to the plates over one day

The two figures above are similar to the figure 5.12 and 5.13, so the same comments can be applied.

Another way to prove that the stratification phenomenon is more pronounced for high tanks than for small ones is to draw the evolution of the temperature profiles for two different cases :

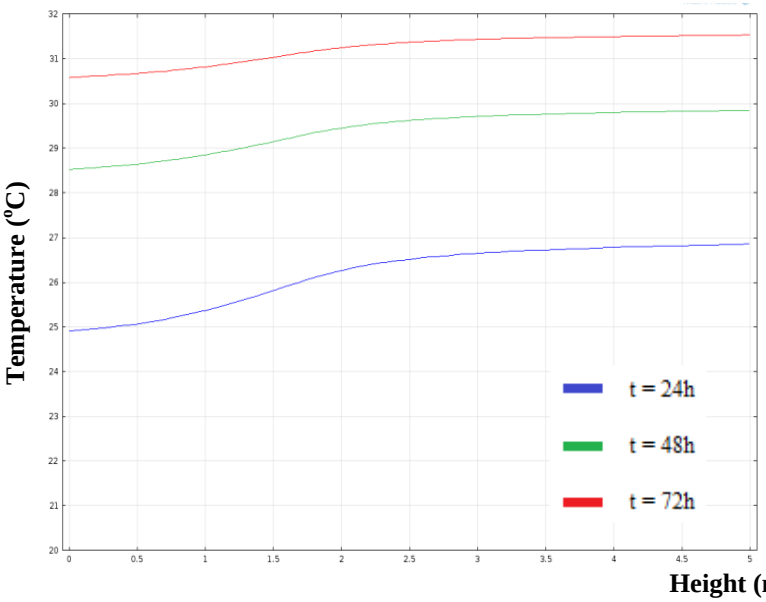

Figure 5.16: Temperature profiles for three times (24h, 48h, 72h) when H=5 m

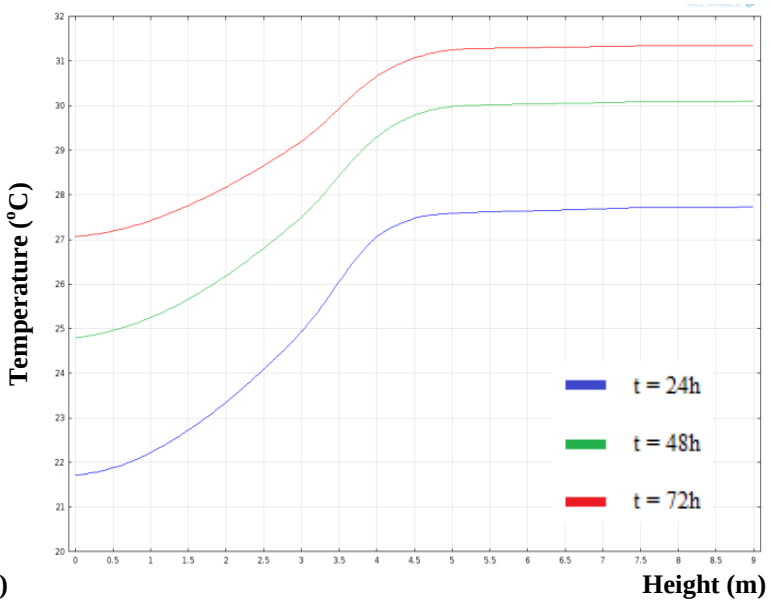

Figure 5.17: Temperature profiles for three times (24h, 48h, 72h) when H=9 m

As shown on the charts above, the temperature profiles for H=5m are less steep than the ones for H=9m. Moreover, the temperature difference between the extremities of the reservoir is higher for the 9m high tank than for the 5 m high tank.

Table 5.3: Temperature difference between the top and the bottom at the center of the tank

	Case 1 : H = 5 m	Case 5 : H = 9 m
ΔT after 24h	2.0°C	6.3°C
ΔT after 48h	1.3°C	5.3°C
ΔT after 72h	1.0°C	4.5°C

The main temperature differences occur for the higher tanks whatever is the time considered. It means that the stratification phenomenon is more pronounced for higher reservoirs than for smaller ones, that is to say the temperature profile is more even within the tank when this one is small.

5.2.3 Input power

To be able to more understand the previous profiles, the focus is now set on the input power involved in each case:

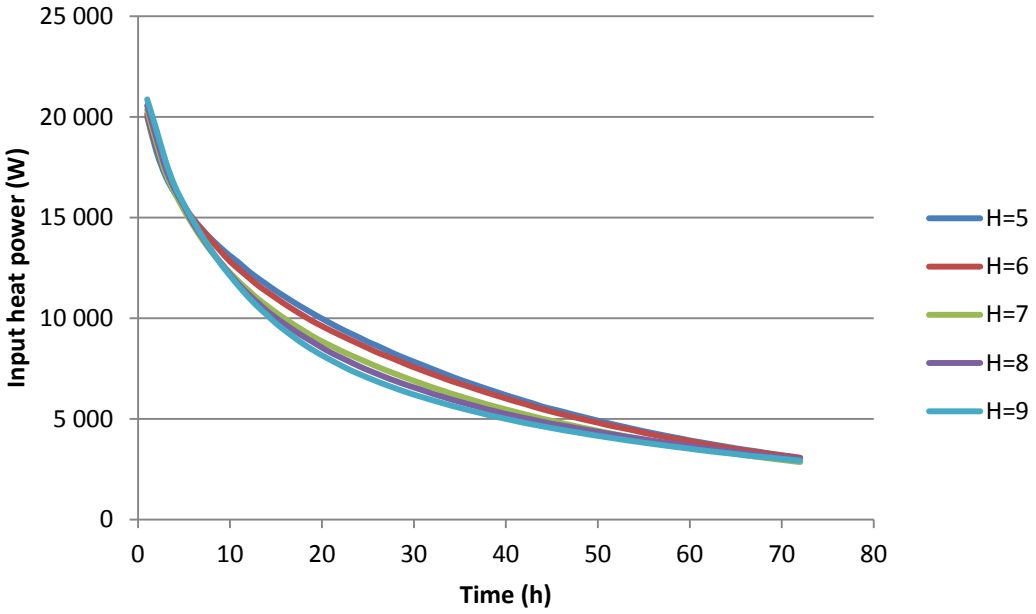

Figure 5.18: Input heat power over the time for the five different cases

The input power for the five cases is in the same magnitude at the start and the end of the simulation, but is slightly different between these two moments. Indeed in between it can be noticed that the smaller the tank, the higher the input power.

To be able to see better what is happening at the beginning of the experiment, a zoom chart is plotted below:

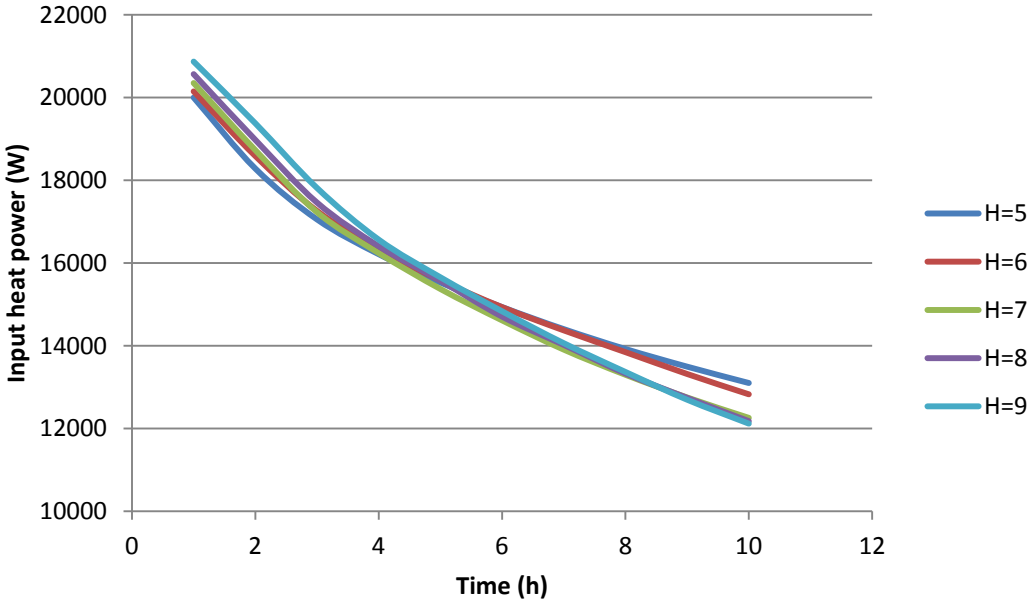

Figure 5.19: Input heat power over the 10 first hours of the simulation for the five different cases

This figure 5.19 above clearly shows what was stated previously, that is to say that at the very beginning of the experiment, the input power is higher for high tanks than for small ones. That is explaining why the temperature evolution in the upper part is faster in high reservoirs than in small ones while the temperature evolution is the same in the bottom part of both high and small tanks. After 5 hours, the trend is reversing since the input power is more important for small tanks and lower for high ones.

Generally speaking, the range of the input power is the same for each case at any time as it can be seen on the figure 5.19. The input power is much higher at the beginning of the simulation than at the end. This is due to a better natural convection at the start of the experiment than at the end. Indeed, when the initial temperature of the water is 20°C, the temperature difference is higher than at any other moment, leading to a natural convection even more important than at the end of the simulation when the temperature of the heat source and the water are close to each other.

5.2.4 Velocity profiles

The two pictures below show the water flow within the tank five hours after the beginning of the simulation:

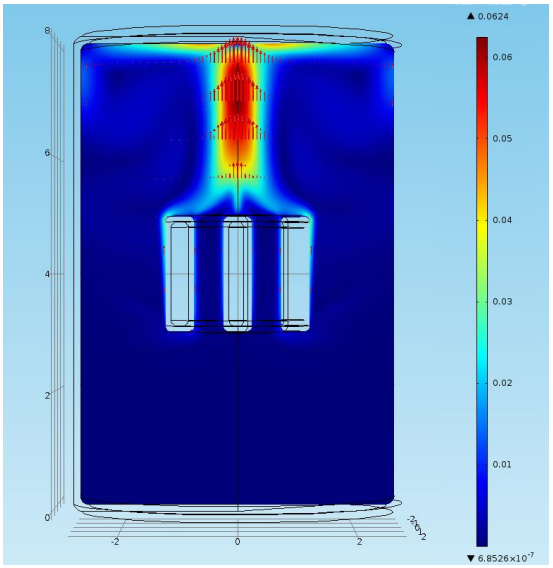

Figure 5.20: Velocity profile after 5h

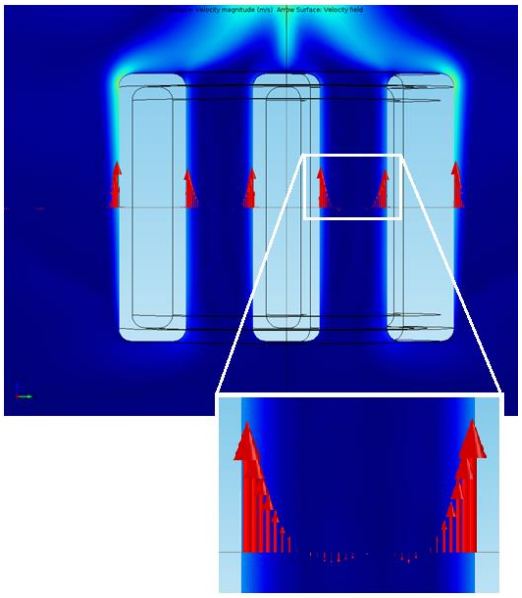

Figure 5.21: Zoom on the velocity profile at the vicinity of the plates after 5h

An upwards flow occurs in the center of the tank whereas downwards flows occur on the edges, creating two symmetrical circular streamlines. The figure 5.21 shows that the flow is going upwards on the edges of the heating plates as the water is warmed up. Generally speaking, the velocity is higher on the edges, close to the plates, than in the water between them.

Drawing the velocity profile allows confirming the results obtained regarding the input power which depends on the convection of water within the tank such as the bigger the convection, the higher the input power. In other words, the velocity of water close to the heating plates has to be important enough in order to improve the heat exchange between the heat source and the water.

To know more precisely what occurs in between the plates, the velocity profiles on a horizontal cut line located between two heating plates are plotted:

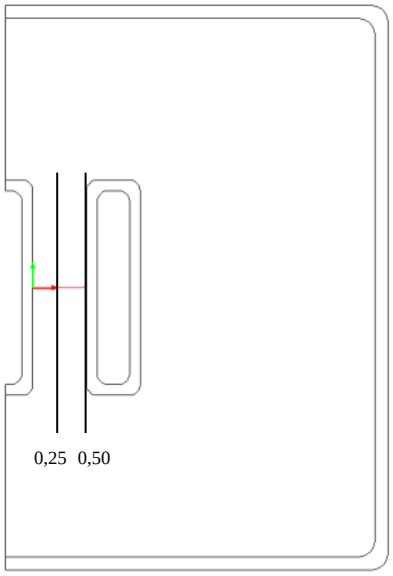

Figure 5.22: Horizontal cut line in between the plates for H=5m

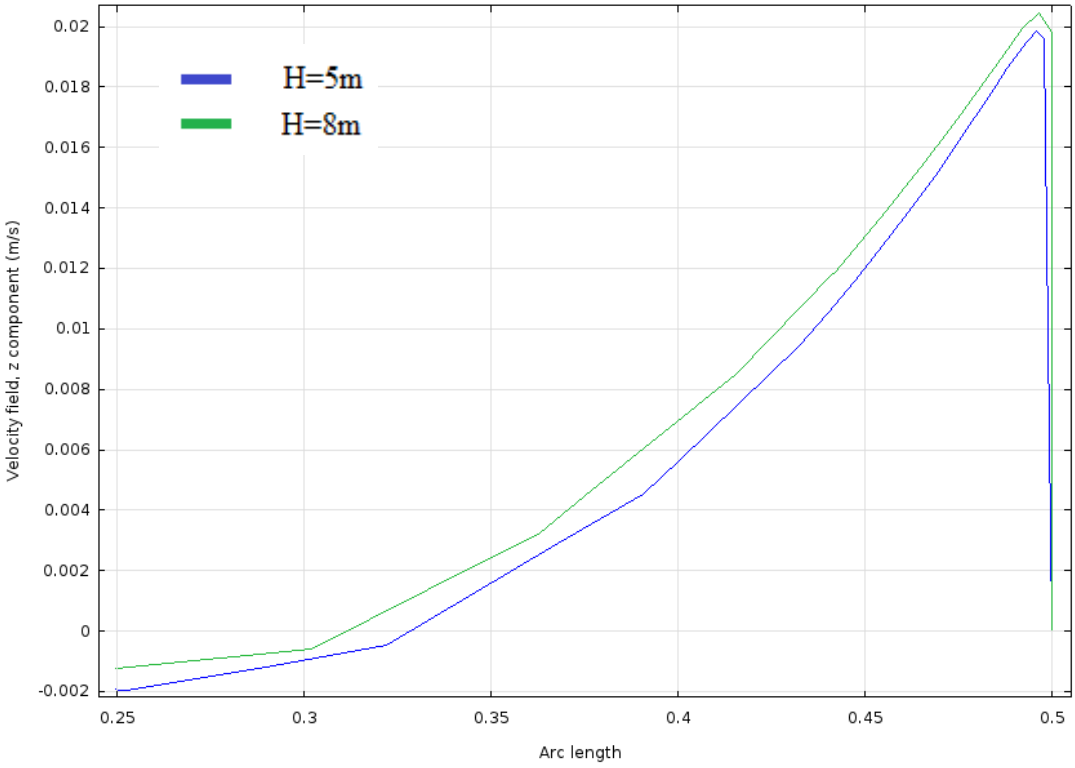

Figure 5.23: Comparison of the velocity profiles in between the plates when H=5m and H=8m after 2 hours

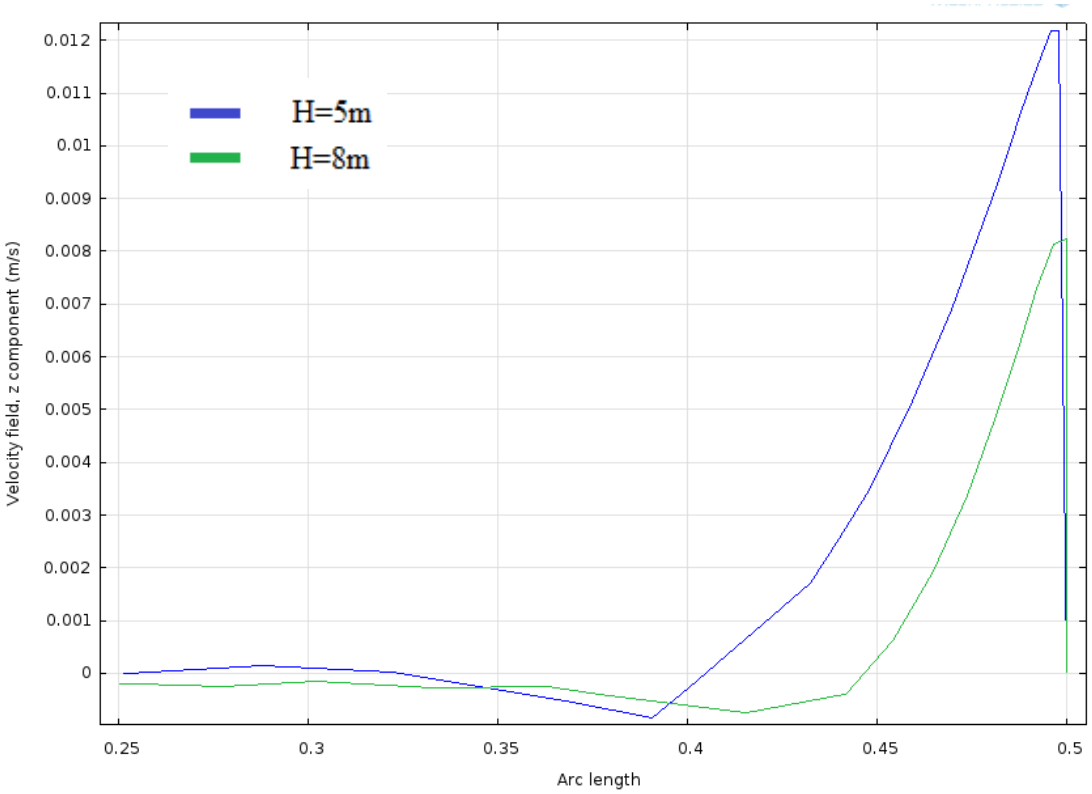

Figure 5.24: Comparison of the velocity profiles in between the plates when H=5m and H=8m after 24 hours

The curves on the figure 5.23 and the figure 5.24 show that the velocity is the highest close to the heating devices and then decreases when being far away from them. The figure 5.24 is correlated with the results obtained about the power as a function of the time since it proves that the average speed over the cut line is higher for the 8 meter high tank than for the 5 meter high tank two hours after the start of the experiment, confirming that the input power is higher for the big reservoir than for the small one at that moment of the simulation.

Once the velocity profile is known in between the plates, it seems also interesting to study it on the edge of the plates for two different heights. To this end, two cut lines are now drawn 1cm next to the central heating device for a 5 and 8 meter high tanks and the velocity profiles are compared:

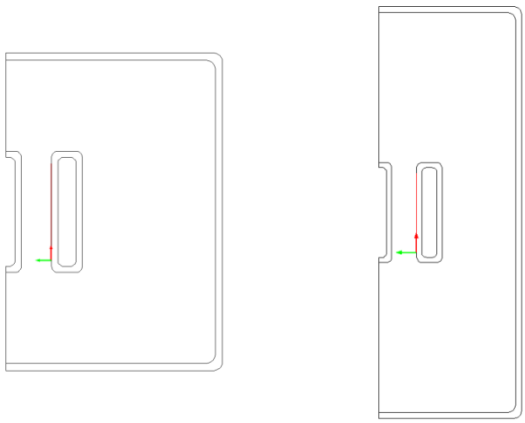

Figure 5.25: Vertical cutline along the plate for H=5m and H=8m

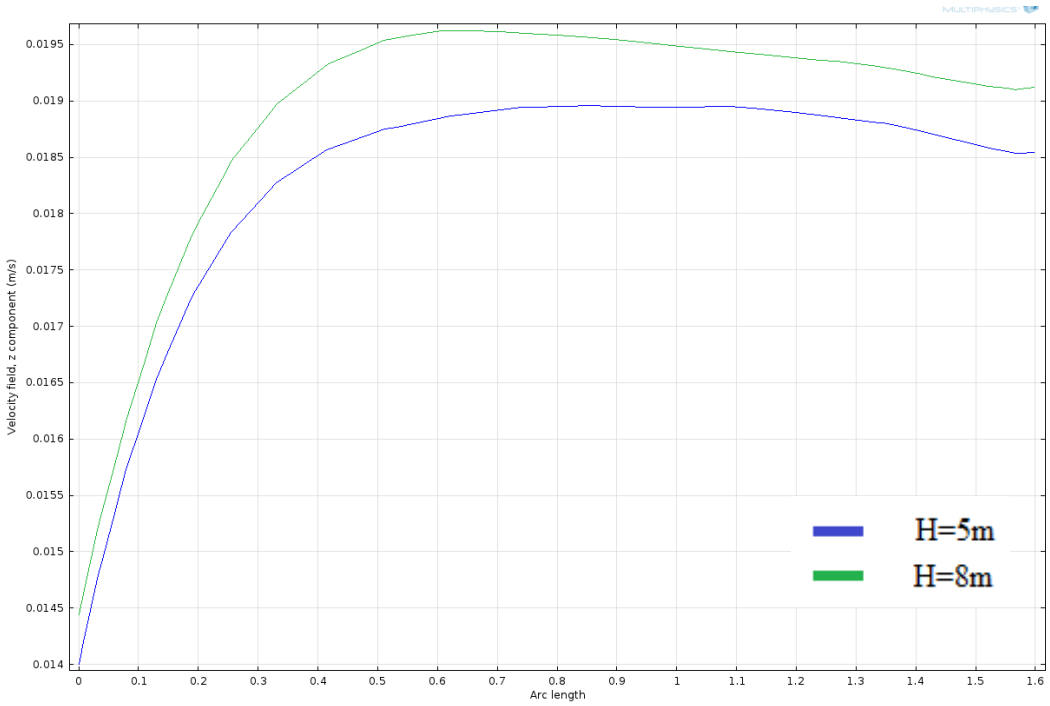

Figure 5.26: Comparison of the velocity profiles along the plate when H=5m and H=8m after 2 hours

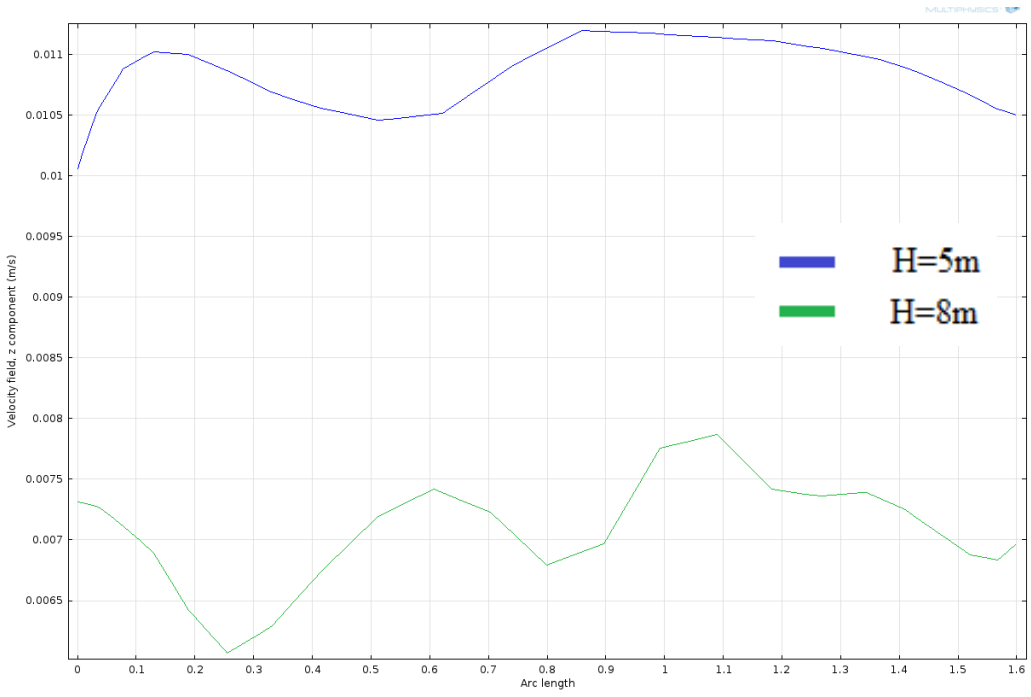

Figure 5.27: Comparison of the velocity profiles along the plate when H=5m and H=8m after 24 hours

The figures 5.26 and 5.27 confirm the results obtained for the input power as a function of the time for each case. Indeed, the figure 5.26 shows that the velocity close to the heating devices for a 8 meter high tank is higher than the one in the 5 meter high tank 2 hours after the start of the simulation. The figure 5.27 confirms that the input power of the 5 meter high tank is higher than the one in the 8 meter high tank after 24 hours since it shows that the velocity of water close to the heating plates is more important for the 5 meter high tank.

CONCLUSION

The purpose of this two-month project work was to investigate the sensible heat storage in order to collect the waste heat released by the supermarket´s refrigerating devices. The temperature distribution within the tank has been studied through combined fluids dynamics and heat transfer computational simulations on COMSOL. The main parameters studied were the location of the heat source and the height of the tank to find out how they can affect the vertical temperature distribution.

Some general conclusions appear from these studies. Indeed, it has been proved that the temperature set for the heat source does not affect significantly the temperature gradient from the bottom towards the top.

Afterwards, the fluid dynamics simulations confirmed that the higher the tank is, the more pronounced the vertical stratification is. Indeed, the driving parameter is the variation of density. Since the effect of the density variation is only observable on the vertical axis, height tanks favor upwards hot water movements as the water is able to easily rise in the vertical direction. On the contrary, water cannot rise so high in smaller tanks and has to transfer its heat also in the horizontal direction. In this way, several temperature layers are created in higher tanks whereas a uniform temperature distribution is apparent in small tanks.

Regarding the heat source location, it has been noticed that a general tendency appears. The temperature gradient from the bottom to the top is the most pronounced when the heat source is placed on the top of the tank whereas the temperature reached is the highest and the most uniform with the heat source on the bottom. On the other hand, putting the heat source in the middle allows creating two distinct temperature layers, one cooler on the bottom part and another one warmer on the top part of the tank. Setting the heat source on the bottom allows having faster the largest amount of hot water available thanks to an efficient free convection and then a high enough input power released. However, the vertical stratification is not ensured during the process. On the contrary, if the heat source is placed on the top, the water tends to stagnate on the top part, which lowers the convection quality and then decreases the input power involved. This enables the vertical temperature distribution to be highly ensured from the bottom to the top. Nevertheless, the amount of hot water available is much lower. Therefore, designing a tank with the heat source in the middle appears like a compromise as it allows having a reasonable amount of hot water quite quickly and the vertical stratification is clearly ensured.

However, which came out from this study is that no universal best solution can be advocated since the choice of the location should be made according to the need. If a large amount of hot water at an even temperature quickly available is needed, then it is better to put the coil on the bottom whereas the coil on the middle enables to draw water at different temperatures.

Finally, sensible heat storage represents an interesting means to collect the heat available from the supermarkets daily usage. The potential in this field is so significant that the supermarkets can be used as a buffer for its surroundings.

APPENDIX A – SPECIFIC HEAT CAPACITIES FOR SEVERAL MATERIALS

In order to more understand why water is one of the most spread storing substances when speaking about sensible heat storage, the values of the specific heat capacity for several common substances have been investigated.

Table A.1: Specific heat capacities for a list of common materials

Materials	Specific heat capacity[xi] Cp (J/kg.K)
Air, dry	1005
Alcohol, ethyl	2440
Aluminum	897
Ammonia, liquid	**4700**
Clay, sandy	1381
Concrete	880
Copper	385
Ice (0°C)	2093
Helium	5193
Hydogen	14304
Iron	449
Oxygen	918
Polypropylene	1920
Polystyrene	1300 - 1500
Polyurethane cast liquid	1800
Polyvinylchloride PVC	840 - 1170
Quartz glass	700
Salt, NaCl	880
Sand, quartz	830
Silver	235
Soil, dry	800
Soil, wet	1480
Snow	2090
Uranium	116
Water, pure liquid (20oC)	**4182**
Water, vapor (27oC)	3985
Wet mud	2512
Wood	1700

Liquid ammonia and liquid water have the highest specific heat. However, as water is non-dangerous and scentless, it is the most used substance for sensible heat storage processes.

APPENDIX B – AVAILABLE HEAT POWER AT THE CONDENSER OVER THE TIME

The first investigations done dealt with the amount of waste heat released by the refrigerating systems. To be accurate, the power shifting hour by hour has been estimated and listed below:

Table B.1: Instantaneous recoverable heat power in January

Hour of the day in January	Instantaneous recoverable heat power (kW)
0	138,45
1	140,38
2	125,76
3	130,19
4	129,79
5	117,78
6	116,40
7	127,34
8	135,99
9	135,46
10	129,41
11	125,56
12	125,47
13	137,92
14	145,70
15	131,93
16	128,64
17	127,07
18	125,89
19	126,97
20	125,17
21	128,75
22	131,38
23	134,34

Table B.2: Instantaneous recoverable heat power in June

Hour of the day in June	Instantaneous recoverable heat power (kW)
0	140,75
1	131,36
2	121,95
3	130,41
4	133,11
5	119,45
6	119,03
7	125,21
8	129,92
9	138,29
10	135,07
11	132,26
12	136,76
13	148,50
14	156,67
15	144,17
16	139,36
17	137,53
18	135,25
19	133,61
20	132,21
21	132,42
22	135,78
23	149,95

Afterwards, in order to have a typical day tendency of the heat power released by month, the average of the instantaneous heat power available is calculated for each hour of all days in a month. The idea is to rebuild the data hour by hour to create a typical day in January for Winter time and in June for Summer time.

The numbers show that every day, the power range is the same depending on the hour of the day. Consequently, it is possible to calculate the tendency for each month. Below are the data for January and June on which the study is based:

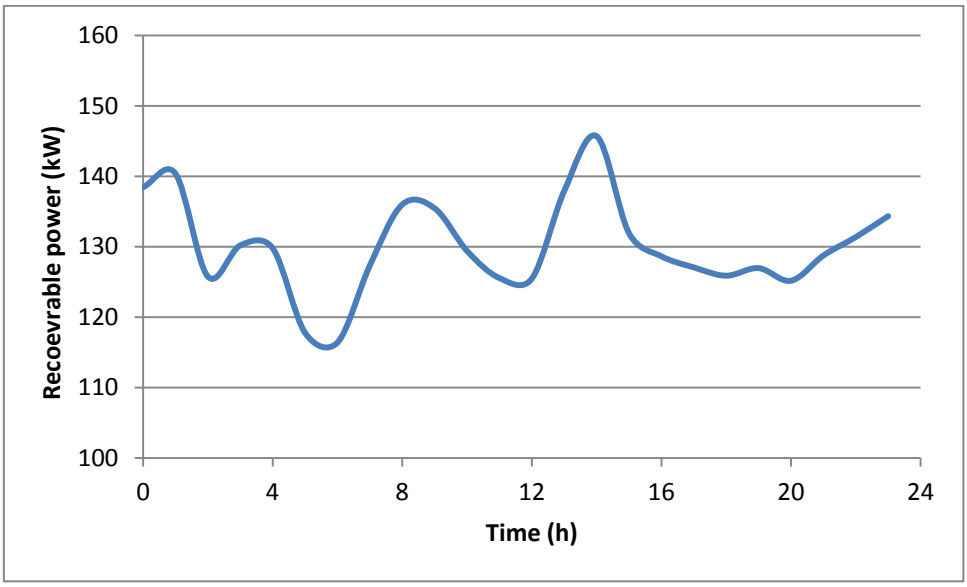

Figure B.1: Tendency of the power rejected from the condensers for a typical day in January

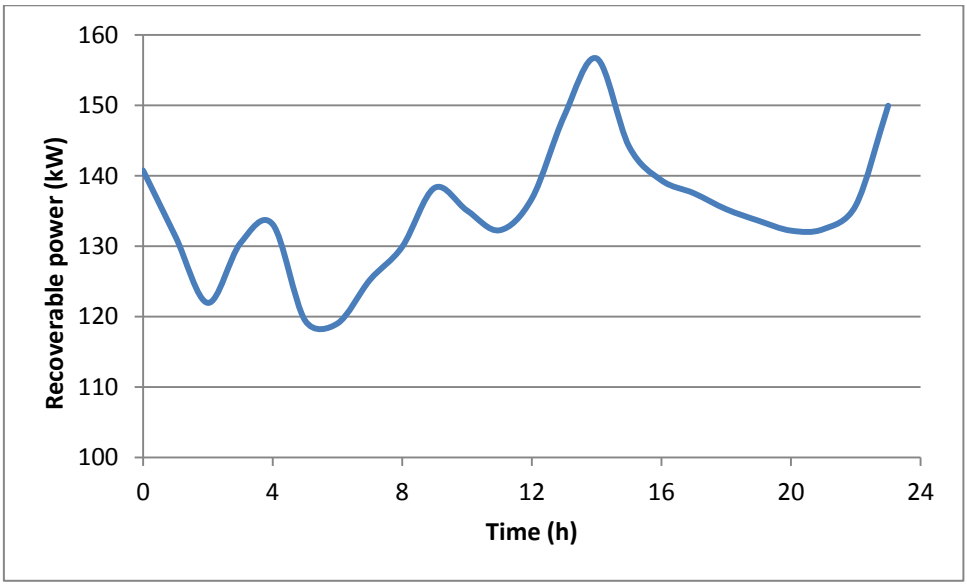

Figure B.2: Tendency of the power rejected from the condensers for a typical day in June

The figures B.1 and B.2 above show that the tendency is the same in January and June. The power span is between 120 kW and 160 kW and the peak consumptions occur almost at the same time. Thus, a constant mean power of 140 kW will be used for the calculations. It should be the input power introduced by the heat source inside the water tank.

However, doing this prevents from taking into account the power shifting during the day. Then, knowing the mean recoverable heat power each day allows to calculate the daily mean recoverable heat energy. Here are the results for both January and June:

Table B.5: Heat recoverable In January and June

Months	Mean recoverable heat power (kW)	Mean recoverable heat energy in a typical day (kWh/day)
January	130	3122
June	135	3239

APPENDIX C – DETERMINATION OF THE OPTIMUM INSULATION LAYER

The tank will be buried near the supermarket´s cooling heat pumps, at around 10m depth where the temperature begins to remain constant. At this depth, the ground temperature set for the outside boundary in the model is T_{ground} = 10°C.

The heat transfer coefficient on the outside shell is h_{ground} = 5,5 W/m^2.K. This value comes from the surface resistance of the ground which equals 0,18 m^2.K/W.

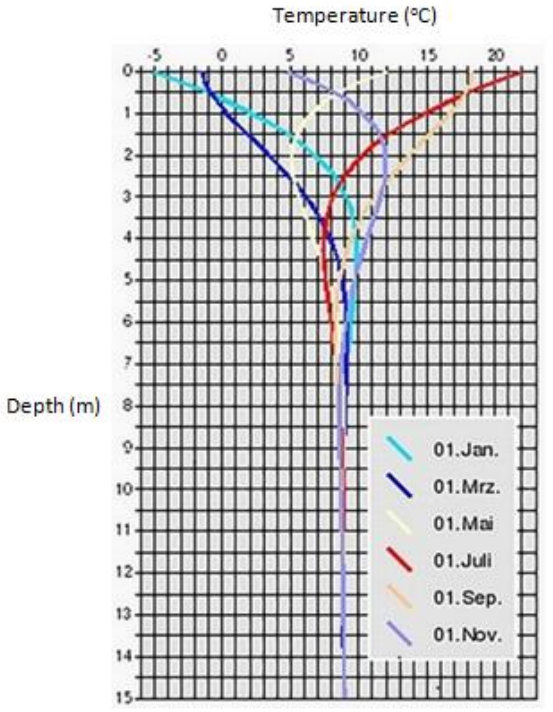

Figure C.1: Ground temperatures as a function of the ground depth

The outside temperature is quite low in comparison with the one inside the tank. That is why to avoid too much heat losses through the shell, the insulation layer should also be estimated. Then the model will get closer to reality.

The properties of the polyurethane foam are used and are given in the table below:

Table C.1: Polyurethane foam insulation layer properties[xii]

	Property	Name	Value	Unit	Property group
✓	Thermal conductivity	k	0.03	W/(m·K)	Basic
✓	Density	rho	50	kg/m^3	Basic
✓	Heat capacity at constant pressure	Cp	1500	J/(kg·K)	Basic

In order to know which thickness range can be the most efficient in this case, the heat flux through the insulation has been studied. As showed on the figure C.2 below, a value seemed to be reached when increasing the thickness does not significantly affect the transfer anymore: this range started at around 12cm.

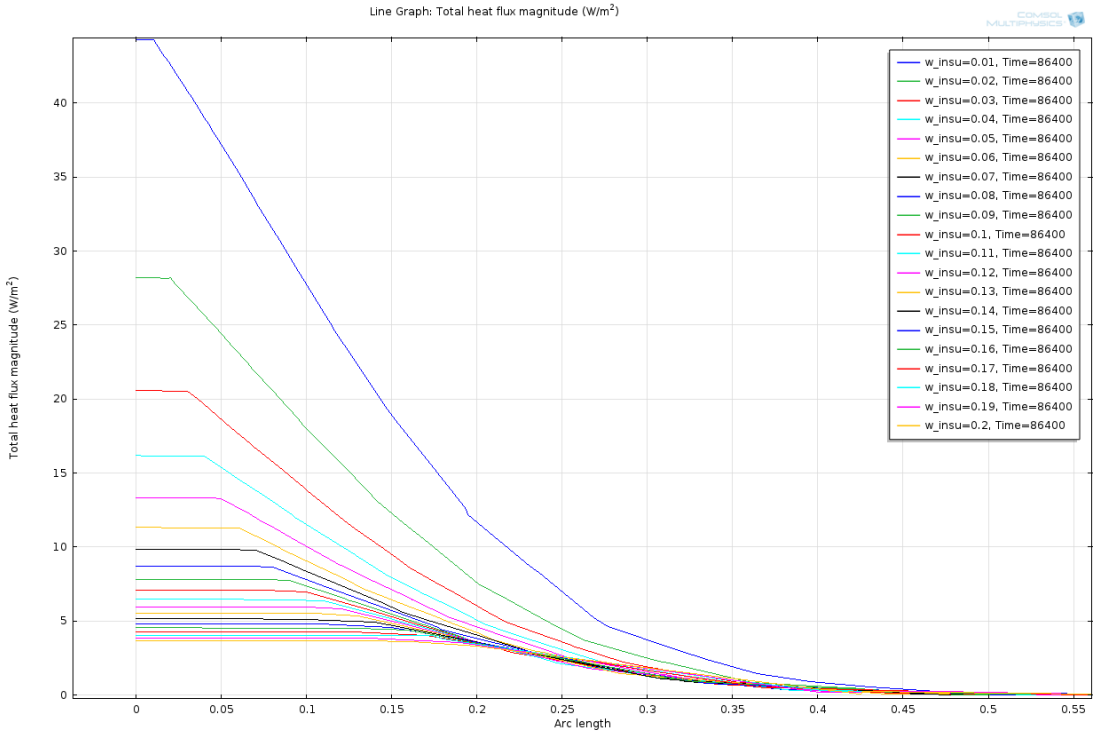

Figure C.2: Evolution of the heat losses flow through the insulated walls as a function of the insulation thickness $W_{insulation}$ [1 ; 20 cm]

Here is the chart representing the heat losses drop when increasing the insulation thickness:

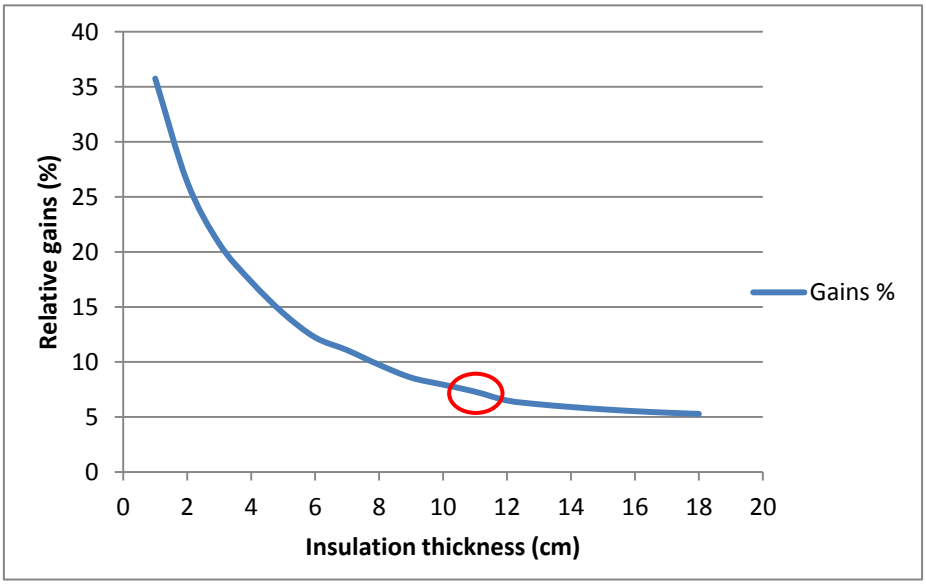

Figure C.3: Relative heat losses gains according to the insulation thickness

At the beginning, increasing the thickness is worth because the gains are still high enough to have real effects on the water temperature inside the tank. However, from 12cm, the heat losses drop becomes very low and the effect of insulation does not seem significant enough.

Thanks to this preliminary study, the optimum insulation thickness is set at 12cm all around the tank.

APPENDIX D – INFLUENCE OF THE HEAT SOURCE TEMPERATURE ON THE STRATIFICATION

General knowledge about heat pump temperatures led to turn towards a low temperature released by the condenser. However, so as to choose the temperature to set to the heat sources, a simulation is done where several temperatures are tried. The parameter T_{heat} has been chosen in a range from 35°C to 50°C with a 5°C step.

Here are the results regarding the temperature evolution on a vertical cut line in the middle of the tank from the bottom to the top after three days:

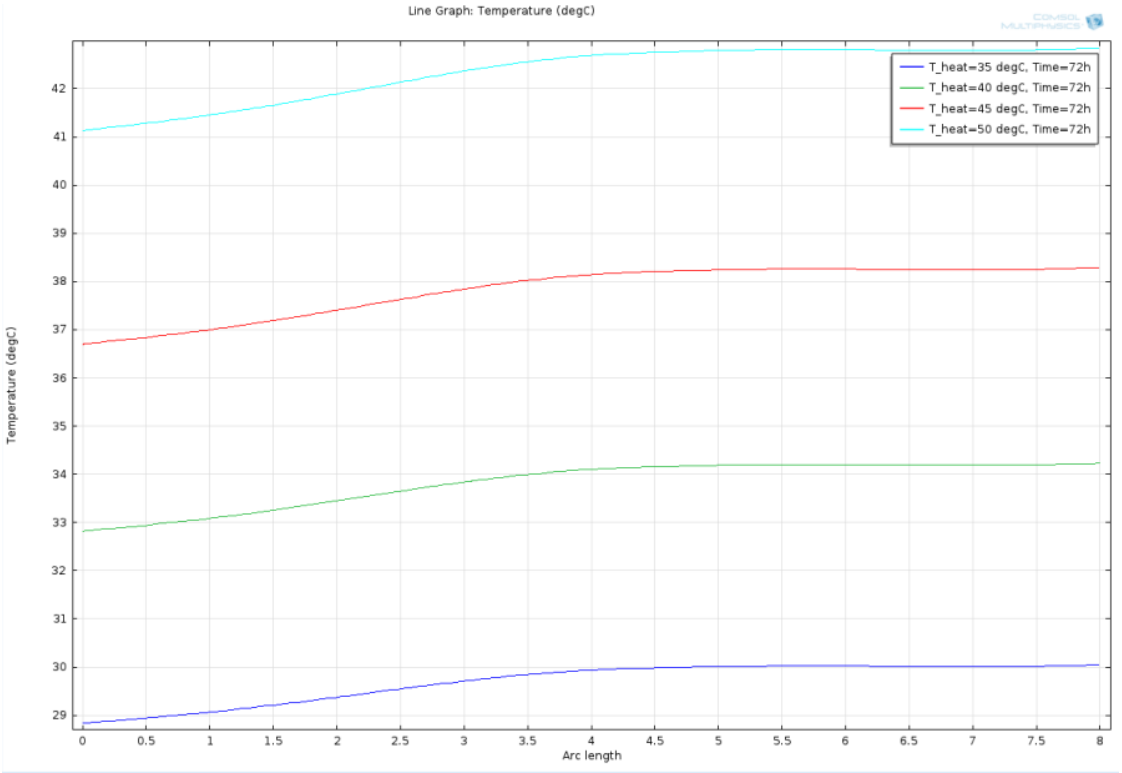

Figure D.1: Temperature profile for different T_{heat} values as a function of the height

It can be noticed that the temperature gradient from the bottom to the top is always a little bit higher when the source is warmer but seems to decrease when the source is 50°C as shown below:

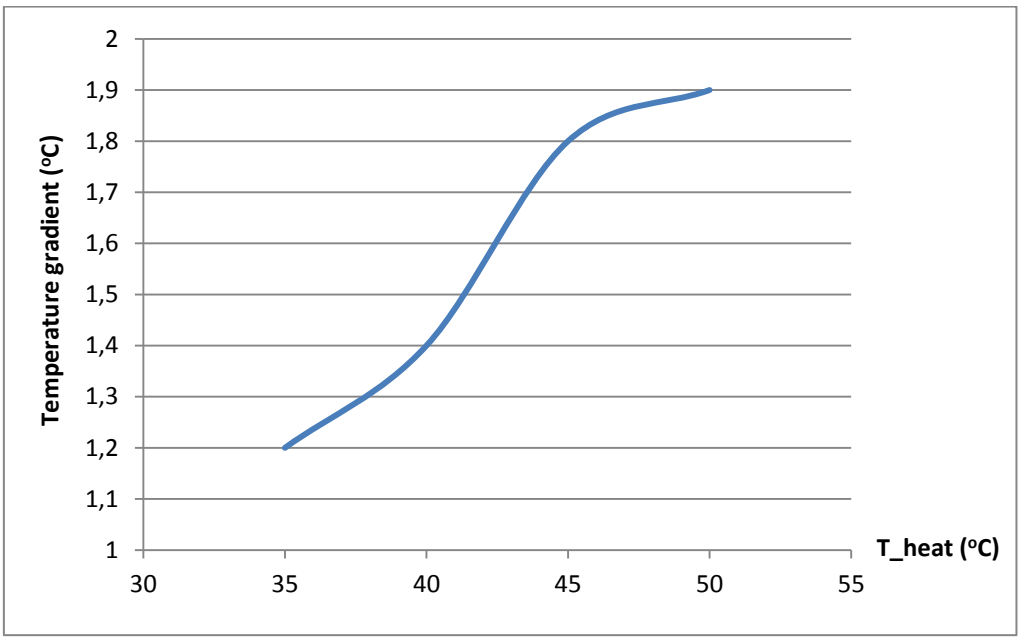

Figure D.2: Temperature gradient according to the heat source temperature set T_{heat}

However, it is obvious that the gradient difference between each case is not so significant, with an average of 0,2°C. Then, none of the cases tested seems to make the difference regarding the temperature gradient reached inside the tank. That is why it is enough to estimate the temperature at the condenser in a specific case assuming the operating characteristics of the heat pump. The detailed process leading to 35°C is developed in the appendix E.

APPENDIX E – STUDY ON THE REFRIGERATING CYCLE FOR THE SETTING OF T_{HEAT} VALUE

As it has been proved that the temperature of the heat source does not affect significantly the temperature distribution within the tank, a specific value has to be set for all the simulations carried out on COMSOL. To this end, the refrigeration cycle is studied assuming that R134A refrigerant is used (Tables C1, C2, C3).

Saturated vapor enters in the compressor at -10°C and the temperature of the refrigerant going out of the condenser is 30°C. The mass flow of refrigerant is 0.08 kg/s. It is also assumed that the pressure of the saturated liquid going out of the condenser is 9 bar and the isentropic efficiencies of the compressor and the condenser are equal to 80%.

All these stages are summarized in the two schemes below:

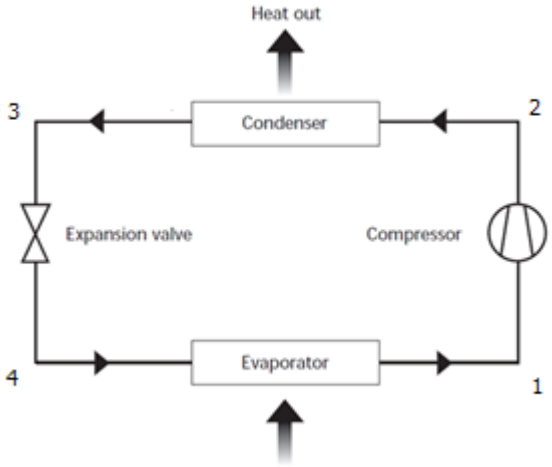

Figure E.1: General refrigerating pump principle

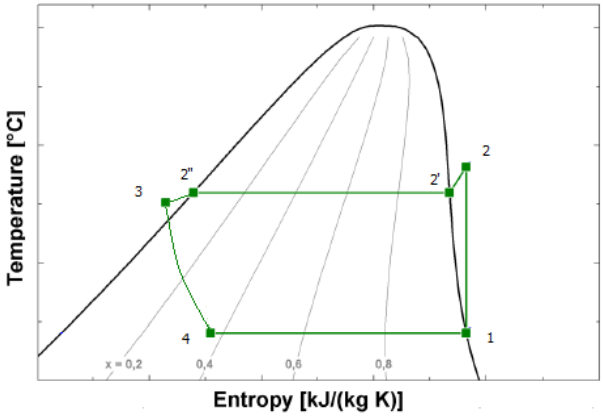

Figure E.2: Temperature-Entropy thermodynamics diagram of the refrigerating pump process

In order to know the refrigerant state and properties at each stage of the process, knowing the assumptions made above, the tables of saturated and superheated R134a refrigerant properties[xiii] are used:

Table C-1: Properties of Saturated R134a, Presented at Regular Intervals of Temperature

Temp. T (°C)	Pressure P (kPa)	Specific volume (m^3/kg)		Specific internal energy (kJ/kg)		Specific enthalpy (kJ/kg)		Specific entropy (kJ/kg-K)		T (°C)
		$10^3 v_f$	v_g	u_f	u_g	h_f	h_g	s_f	s_g	
-40	51.25	0.7053	0.36064	-0.04	207.38	0.00	225.86	0.0000	0.9687	-40
-35	66.19	0.7126	0.28373	6.25	210.25	6.29	229.03	0.0267	0.9619	-35
-30	84.43	0.7201	0.22577	12.58	213.12	12.64	232.19	0.0530	0.9559	-30
-25	106.5	0.7280	0.18152	18.95	215.99	19.03	235.32	0.0789	0.9505	-25
-20	132.8	0.7361	0.14735	25.37	218.86	25.47	238.43	0.1046	0.9457	-20
-15	164.0	0.7445	0.12066	31.85	221.72	31.97	241.51	0.1299	0.9415	-15
-10	200.7	0.7533	0.09960	38.38	224.56	38.53	244.55	0.1550	0.9378	-10
-5	243.5	0.7625	0.08282	44.96	227.38	45.15	247.55	0.1798	0.9345	-5
0	293.0	0.7722	0.06934	51.61	230.18	51.83	250.50	0.2043	0.9316	0
5	349.9	0.7823	0.05840	58.31	232.96	58.59	253.39	0.2287	0.9290	5
10	414.9	0.7929	0.04947	65.09	235.69	65.42	256.22	0.2528	0.9266	10
15	488.7	0.8041	0.04211	71.93	238.39	72.32	258.97	0.2768	0.9245	15
20	572.1	0.8160	0.03601	78.85	241.04	79.32	261.64	0.3006	0.9225	20
25	665.8	0.8286	0.03092	85.85	243.64	86.40	264.23	0.3243	0.9207	25
30	770.6	0.8421	0.02665	92.93	246.17	93.58	266.71	0.3479	0.9190	30
35	887.5	0.8565	0.02304	100.11	248.63	100.87	269.08	0.3714	0.9173	35
40	1017	0.8720	0.01997	107.39	251.00	108.28	271.31	0.3949	0.9155	40
45	1161	0.8889	0.01734	114.79	253.27	115.82	273.40	0.4184	0.9137	45
50	1319	0.9072	0.01509	122.30	255.42	123.50	275.32	0.4419	0.9117	50
55	1492	0.9274	0.01314	129.96	257.43	131.35	277.03	0.4655	0.9095	55
60	1688	0.9498	0.01144	137.79	259.25	139.38	278.51	0.4893	0.9069	60
65	1891	0.9751	0.00996	145.80	260.86	147.64	279.69	0.5133	0.9038	65
70	2118	1.0038	0.00865	154.04	262.20	156.16	280.52	0.5377	0.9000	70
75	2366	1.0372	0.00749	162.54	263.17	165.00	280.88	0.5625	0.8953	75
80	2635	1.0774	0.00644	171.43	263.66	174.27	280.63	0.5881	0.8893	80
85	2928	1.1273	0.00548	180.81	263.45	184.11	279.51	0.6149	0.8812	85
90	3247	1.1938	0.00459	190.94	262.13	194.82	277.04	0.6435	0.8699	90
95	3594	1.2945	0.00371	202.49	258.73	207.14	272.08	0.6760	0.8524	95
100	3975	1.5269	0.00266	218.73	248.46	224.80	259.02	0.7222	0.8139	100
101.03	4059	1.9685	0.0019685	232.95	233.90	241.88	241.88	0.7678	0.7678	101.03

Table C-2: Properties of Saturated R134a, Presented at Regular Intervals of Pressure

Pressure P (kPa)	Temp. T (°C)	Specific volume (m^3/kg)		Specific internal energy (kJ/kg)		Specific enthalpy (kJ/kg)		Specific entropy (kJ/kg-K)		P (kPa)
		$10^3 v_f$	v_g	u_f	u_g	h_f	h_g	s_f	s_g	
40	-44.61	0.699	0.45483	-5.79	204.74	-5.76	222.94	-0.0249	0.9757	40
60	-36.95	0.710	0.31108	3.79	209.13	3.84	227.80	0.0163	0.9644	60
80	-31.13	0.718	0.23749	11.14	212.48	11.20	231.47	0.0471	0.9572	80
100	-26.37	0.726	0.19255	17.19	215.21	17.27	234.46	0.0718	0.9519	100
200	-10.09	0.753	0.09995	38.26	224.51	38.41	244.50	0.1545	0.9379	200
300	0.65	0.773	0.06778	52.48	230.55	52.71	250.88	0.2075	0.9312	300
400	8.91	0.791	0.05127	63.61	235.10	63.92	255.61	0.2476	0.9271	400
500	15.71	0.806	0.04117	72.92	238.77	73.32	259.36	0.2802	0.9242	500
600	21.55	0.820	0.03433	81.01	241.86	81.50	262.46	0.3080	0.9220	600
700	26.69	0.833	0.02939	88.24	244.51	88.82	265.08	0.3323	0.9201	700
800	31.31	0.846	0.02565	94.80	246.82	95.48	267.34	0.3541	0.9185	800
900	35.51	0.858	0.02270	100.84	248.88	101.62	269.31	0.3738	0.9171	900
1000	39.37	0.870	0.02033	106.47	250.71	107.34	271.04	0.3920	0.9157	1000
1200	46.29	0.893	0.01673	116.72	253.84	117.79	273.92	0.4245	0.9132	1200
1400	52.40	0.917	0.01412	125.96	256.40	127.25	276.17	0.4532	0.9107	1400
1600	57.88	0.940	0.01213	134.45	258.50	135.96	277.92	0.4792	0.9080	1600
1800	62.87	0.964	0.01057	142.36	260.21	144.09	279.23	0.5030	0.9052	1800
2000	67.45	0.989	0.00930	149.81	261.56	151.78	280.15	0.5252	0.9020	2000
2200	71.70	1.015	0.00824	156.90	262.57	159.13	280.70	0.5460	0.8985	2200
2400	75.66	1.042	0.00734	163.70	263.27	166.20	280.89	0.5658	0.8946	2400
2600	79.37	1.072	0.00657	170.29	263.63	173.08	280.70	0.5848	0.8901	2600
2800	82.86	1.104	0.00588	176.73	263.64	179.82	280.11	0.6033	0.8849	2800
3000	86.16	1.141	0.00527	183.09	263.26	186.51	279.08	0.6213	0.8789	3000
3200	89.29	1.182	0.00472	189.41	262.41	193.19	277.50	0.6392	0.8718	3200
3400	92.26	1.233	0.00420	195.91	260.96	200.10	275.23	0.6575	0.8631	3400
3600	95.08	1.297	0.00370	202.66	258.65	207.32	271.97	0.6765	0.8521	3600
3800	97.76	1.387	0.00319	210.26	254.87	215.54	266.99	0.6980	0.8367	3800
4000	100.31	1.562	0.00256	220.43	246.82	226.68	257.05	0.7272	0.8085	4000
4059	101.03	1.9685	0.0019685	232.95	233.90	241.88	241.88	0.7678	0.7678	4059

Table C-3 (continued): Properties of Superheated Vapor: Pressures from 500 kPa to 1.3 MPa

P (kPa)		Temperature, T (°C)										
		20	30	40	50	60	70	80	900	100	110	120
500	v (m³/kg)	0.0421	0.0443	0.0465	0.0485	0.0505	0.0524	0.0543	0.0562	0.0580	0.0599	0.0617
	u (kJ/kg)	242.4	250.9	259.3	267.7	276.3	284.9	293.7	302.5	311.5	320.6	329.9
	h (kJ/kg)	263.5	273.0	282.5	292.0	301.5	311.1	320.8	330.6	340.5	350.6	360.8
	s (kJ/kg-K)	0.9384	0.9704	1.001	1.031	1.06	1.088	1.116	1.144	1.171	1.197	1.223
600	v (m³/kg)		0.0360	0.0379	0.0397	0.0414	0.0431	0.0447	0.0463	0.0479	0.0494	0.051
	u (kJ/kg)		249.2	257.9	266.5	275.2	283.9	292.7	301.7	310.7	319.9	329.2
	h (kJ/kg)		270.8	280.6	290.3	300.0	309.8	319.6	329.5	339.5	349.6	359.8
	s (kJ/kg-K)		0.95	0.9817	1.012	1.042	1.071	1.099	1.126	1.154	1.18	1.207
700	v (m³/kg)		0.0300	0.0317	0.0333	0.0349	0.0364	0.0378	0.0393	0.0406	0.0420	0.0434
	u (kJ/kg)		247.5	256.4	265.2	274.0	282.9	291.8	300.8	310	319.2	328.6
	h (kJ/kg)		268.5	278.6	288.5	298.4	308.3	318.3	328.3	338.4	348.6	358.9
	s (kJ/kg-K)		0.9314	0.9642	0.9955	1.026	1.055	1.084	1.112	1.139	1.166	1.192
800	v (m³/kg)			0.0270	0.0286	0.0300	0.0313	0.0327	0.0339	0.0352	0.0364	0.0376
	u (kJ/kg)			254.8	263.9	272.8	281.8	290.9	300.0	309.2	318.5	327.9
	h (kJ/kg)			276.5	286.7	296.8	306.9	317	327.1	337.3	347.6	358.0
	s (kJ/kg-K)			0.9481	0.9803	1.011	1.041	1.07	1.098	1.126	1.153	1.18
900	v (m³/kg)			0.0234	0.02481	0.0262	0.0274	0.0286	0.0298	0.0310	0.0321	0.0332
	u (kJ/kg)			253.2	262.5	271.6	280.7	289.9	299.1	308.4	317.7	327.2
	h (kJ/kg)			274.2	284.8	295.1	305.4	315.6	325.9	336.2	346.6	357.0
	s (kJ/kg-K)			0.9328	0.9661	0.9977	1.028	1.057	1.086	1.114	1.141	1.168
1000	v (m³/kg)			0.0204	0.0218	0.0231	0.0243	0.0254	0.0265	0.0276	0.0286	0.0296
	u (kJ/kg)			251.3	261.0	270.3	279.6	288.9	298.2	307.5	317.0	326.5
	h (kJ/kg)			271.7	282.8	293.4	303.9	314.3	324.7	335.1	345.5	356.1
	s (kJ/kg-K)			0.918	0.9526	0.9851	1.016	1.046	1.075	1.103	1.131	1.158
1100	v (m³/kg)				0.0193	0.0205	0.0217	0.0228	0.0238	0.0248	0.0257	0.0267
	u (kJ/kg)				259.4	269.0	278.4	287.8	297.2	306.7	316.2	325.8
	h (kJ/kg)				280.6	291.6	302.3	312.9	323.4	333.9	344.5	355.1
	s (kJ/kg-K)				0.9396	0.973	1.005	1.035	1.065	1.093	1.121	1.148
1200	v (m³/kg)				0.0172	0.0184	0.0195	0.0205	0.0215	0.0224	0.0234	0.0242
	u (kJ/kg)				257.6	267.6	277.2	286.8	296.3	305.8	315.4	325.1
	h (kJ/kg)				278.3	289.7	300.6	311.4	322.1	332.7	343.4	354.1
	s (kJ/kg-K)				0.9268	0.9615	0.9939	1.025	1.055	1.084	1.112	1.139
1300	v (m³/kg)				0.0154	0.0166	0.0177	0.0187	0.0196	0.0205	0.0213	0.0222
	u (kJ/kg)				255.8	266.1	276.0	285.7	295.3	304.9	314.6	324.3
	h (kJ/kg)				275.8	287.6	298.9	309.9	320.8	331.5	342.3	353.1
	s (kJ/kg-K)				0.914	0.9501	0.9835	1.015	1.045	1.075	1.103	1.131
P (kPa)		20	30	40	50	60	70	80	900	100	110	120
		Temperature, T (°C)										

Here are the refrigerant properties at each stage of the cycle:

Table E.1: Values of the thermodynamics parameters involved at each point of the cycle

Point on the cycle	T (°C)	P (bar)	h (kJ/kg)
1	-10	2.01	241.35
2	48.03	9	280.15
2’	35.5	9	269.3
2’’	35.5	9	101.6
3	30	9	91.49
4	-10	2.01	91.49

The refrigerant enters in the condenser as vapor, then it is saturated and turns into liquid before leaving the condenser. It is calculated that 89% of the transformation occurs with a saturated refrigerant at 35.5°C. Indeed, the enthalpy difference between the inlet and the outlet of the condenser is equal to 188,5 kJ/kg whereas the enthalpy difference between the saturated vapor point and the saturated liquid point is equal to 167,7 kJ/kg.

APPENDIX F – TOWARDS THE STUDY WHEN ADDING AN INLET OF HOT WATER

The idea was to study the temperature distribution within the tank when an inlet of hot water is installed in the tank. In other words, the heat source would have been removed from the reservoir and placed outside, heating directly the water injected inside the tank.

The first simulations that have been run as a turbulent model led to error messages from COMSOL that have not been solved whereas there was no problem when running the simulation with a laminar model. As a consequence, it was investigated how close were the results when simulating with a turbulent model and a laminar one. The model used for these simulations was a 8 meter high tank with three heating plates in the middle. In order to compare the results, two vertical cut lines have been drawn, between the heating devices and on the side of the tank:

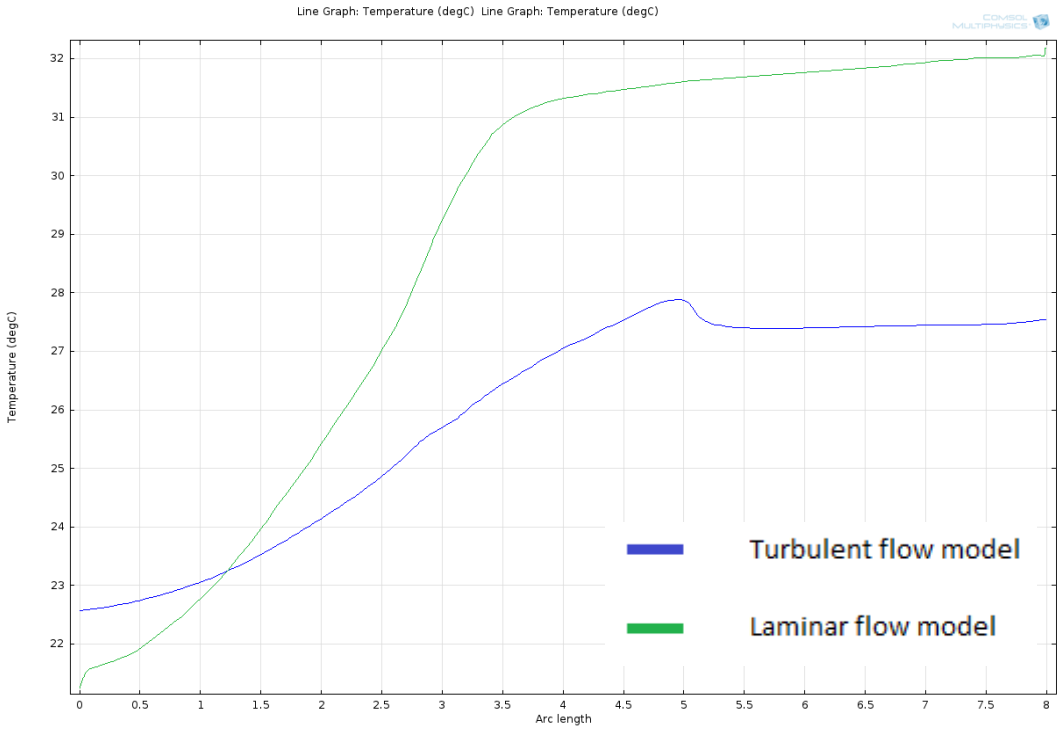

Figure F.1: Comparison of the temperature distribution on the central cutline for a turbulent and a laminar simulation

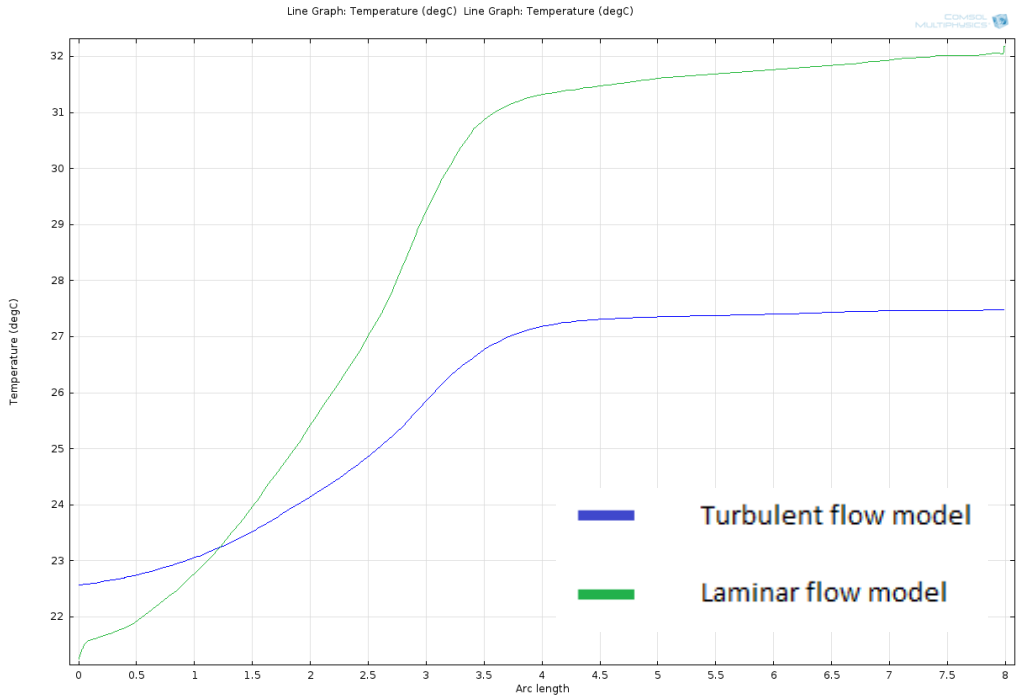

Figure F.2: Comparison of the temperature distribution on the central cutline for a turbulent and a laminar simulation

These two charts show that the temperature profiles are completely different when simulating a turbulent and a laminar flow. The figure F.3 below proves that the temperature distribution within the tank cannot be identical since the input powers of both cases are different at any time.

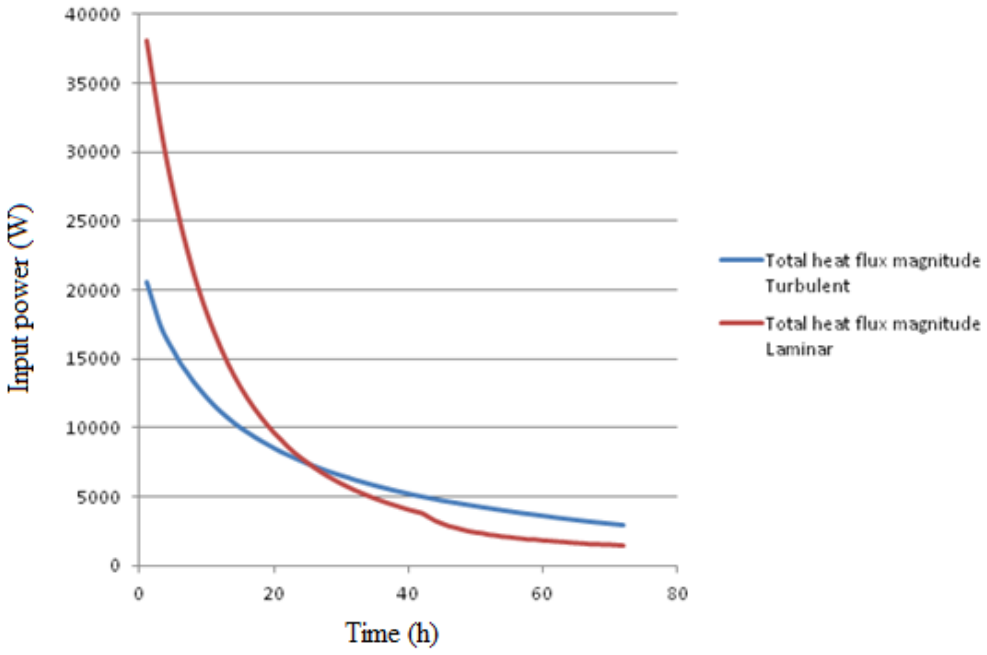

Figure F.3: Comparison of the input power for a turbulent and a laminar simulation

Consequently, as the results are not even close to each other, the approximation of simulating the inlet of hot water within the tank with a laminar model cannot be done, otherwise the results would be completely false.

BIBLIOGRAPHY

Arias, J., (2005): *Energy Usage in Supermarkets – Modelling and Field Measurements*. PhD Thesis. Department of Energy Technology, Royal Institute of Technology, Publication No. 05/45, Stockholm, Sweden, 2005
http://www.diva-portal.org/smash/get/diva2:7929/FULLTEXT01.pdf

Van Reener, D., (2011): *Modelling the performance of underground heat exchangers and storage systems*. Master´s thesis. Department of Civil and Environmental Engineering, Chalmers University of Technology, Publication No. 2011:83, Göteborg, Sweden, 2011

Dai, Y.J., Han, Y.M., Wang, R.Z., (2008): Thermal stratification within the water tank. *Renewable and Sustainable Energy Reviews 13*, 1014-1026, 2009
www.elsevier.com/locate/rser

Wrobel, J., W.Jack, M., (2008): Thermodynamic optimization of a stratified thermal storage device. *Applied Thermal Engineering 29*, 2344-2349, 2009
www.elsevier.com/locate/apthermeng

Dang-Soon, J., Hey-Suk, K., Hyung-Gi, Y., Mi-Soo, S., Sang-Nam, L., Young-Soo, L., (2003): Numerical and experimental study on the design of a stratified thermal storage system. *Applied Thermal Engineering 24*, 17-27, 2004
www.elsevier.com/locate/apthermeng

Levers, S., Lin, W., (2009): Numerical simulation of three-dimensional flow dynamics in a hot water storage tank. *Applied Energy 86*, 2604-2614, 2009
www.elsevier.com/locate/apenergy

REFERENCES

[i] Data Hannover supermarket
https://www.frigodata.net/
Historie – ECO XP REWE 5573 Hannover Wettbergen

[ii] Ground surface resistance:
http://herve.silve.pagesperso-orange.fr/deperditions/deperd_rt.htm

[iii] Vapor compression process
http://www.designbuilder.co.uk/helpv3.1/Content/Detailed_HVAC/Pre_defined_Condenser_Loop.htm
http://ninjacraze.hubpages.com/hub/What-is-Vapour-Compression-Refrigeration-System

[iv] Physical characteristics for water:
http://www.thermexcel.com/french/tables/eau_atm.htm
http://www.engineeringtoolbox.com/absolute-dynamic-viscosity-water-d_575.html

[v] COMSOL database Model: models.cfd.displacement_ventilation.pdf

[vi] Value from thermal expansion of water
http://physchem.kfunigraz.ac.at/sm/Service/Water/H2Othermexp.htm

[vii] Critical Grashof for turbulent flow
https://www.princeton.edu/~achaney/tmve/wiki100k/docs/Grashof_number.html

[viii] k-ε turbulent flow model
http://www.cfd-online.com/Wiki/K-epsilon_models

[ix] Ground temperatures
http://guidebatimentdurable.bruxellesenvironnement.be/fr/g-ene07-appliquer-une-strategie-de-refroidissement-passif.html?IDC=22&IDD=5981

[x] Heat equation
http://www.es.ucsc.edu/~fnimmo/website/temperature.pdf

[xi] Specific heat capacities for several substances
http://www.engineeringtoolbox.com/specific-heat-capacity-d_391.html

[xii] Thermal properties of polyurethane
http://www.excellence-in-insulation.eu/site/fileadmin/user_upload/PDF/Thermal_insulation_materials_made_of_rigid_polyurethane_foam.pdf

[xiii] Property tables for R134a refrigerant
http://www.google.fr/url?sa=t&rct=j&q=&esrc=s&source=web&cd=1&ved=0CC4QFjAA&url=http%3A%2F%2Fwww.cambridge.org%2Fve%2Fdownload_file%2F212553%2F&ei=VXI5U8z9GofOygPOmYBg&usg=AFQjCNFQ26ojIYke0z9EWjLLNPEynHiuNA&bvm=bv.63808443,d.bGQ